$CD4^+$ T cells, on activation and expansion, develop into different Th cell subsets with different cytokine profiles and distinct effector functions. Th17 cells are the newest member of the effector Th cell family and are characterized by their ability to produce specific cytokines such as IL-17, IL-22, IL-17F, IL-21, and CCL20. TGF-β, IL-6, IL-1β, IL-21, and IL-23 are important for the polarization of Th17 cells from human $CD4^+$ naive T cells (20, 21), and the absence of TGF-β mediates a shift from a Th17 profile to a Th1 profile (21, 22). Recent studies have demonstrated that Th17 cells, rather than Th1 cells, play a pivotal role in the pathogenesis of autoimmune disease models, including experimental autoimmune encephalomyelitis (EAE) and collagen-induced arthritis (23, 24). Furthermore, a number of observations suggest that Th17 cytokines may be important in rheumatoid arthritis (RA), a representative human autoimmune inflammatory disease. IL-17 is found in RA synovial fluid and in the T cell-rich areas of RA synovial tissue (25–28). In RA patients, in a 2-y prospective study, the cytokine expression of TNF-α, IL-1β, and IL-17 was predictive of joint destruction, whereas IFN-γ was protective (29). Although the direct proinflammatory effects of IL-17 are often small when compared with those of IL-1β and TNF-α, IL-17 may enhance the effects of other cytokines. Using RA synovial tissue fibroblasts, IL-17 enhanced IL-1–mediated IL-6 and CCL20 production (30, 31) and the TNF-α–induced synthesis of IL-1β, IL-6, IL-8, and CCL20 (31, 32), indicating that the effects of IL-17 may be caused by its ability to promote inflammation by inducing cytokines and chemokines (33, 34). Furthermore, direct effector functions of Th17 cells in RA have been demonstrated in that receptor activator for NF-κB ligand (RANKL) expression on the surface of Th17 cells induces osteoclastogenesis (25, 35, 36), promoting cartilage and bone destruction independently of TNF-α and IL-1β (37, 38). These proinflammatory cytokines induced by IL-17 might even feedback on the generation and expansion of further Th17 cells in this specific microenvironment of the joint. Actually, initial observations from phase I trials show that signs and symptoms of RA are significantly suppressed after treatment with anti–IL-17 Abs, without notable adverse effects, indicating that IL-17 is an important therapeutic target for the treatment of RA (39).

Dendritic cells (DCs) are the most powerful APCs that determine the balance of differentiation of Th cell subsets. In particular, cytokines produced by DCs are regarded as the key to T cell differentiation. For example, IL-12 produced by DCs induces the differentiation to Th1 (40). In our previous studies, we showed that human monocyte-derived DCs stored dopamine, and that dopamine was released on Ag-specific interaction with naive $CD4^+$ T cells (41). Furthermore, antagonizing dopamine receptor subtypes differentially affected Th17 polarization in vitro (19). D2-like receptor antagonists judged to be Th17 adjuvants in vitro caused a marked deterioration of EAE, whereas D1-like receptor antagonists exhibited a marked improvement in EAE (19). Although the precise mechanism of how D1-like receptor antagonists inhibit IL-17 production remains undetermined, our previous results indicated that DC-derived dopamine might induce the differentiation to Th17.

In this study, we show that dopamine induces IL-6–dependent IL-17 production in vitro, and that antagonizing D1-like receptor inhibits dopamine-mediated IL-6–Th17 axis in vitro and in a human RA/SCID mouse chimera model.

Materials and Methods

Purification of human naive $CD4^+$ T lymphocytes

The study using peripheral blood of healthy volunteers was approved by the Human Subjects Research Committee of the University of Occupational and Environmental Health, Japan. Highly purified, untouched $CD4^+$ T cells were prepared from PBMCs of healthy volunteers by exhaustive immunomagnetic negative selection. We routinely used AutoMACS separation columns (Miltenyi Biotec, Germany) and a $CD4^+$ T cell Isolation Kit II (Miltenyi Biotec), and separated into $CD45RO^+$ memory T cells and $CD45RA^+$ naive T cells using $CD45RO^+$ MicroBeads (Miltenyi Biotec). A FACSCalibur flow cytometer (BD Biosciences) showed the purity of these cells to be >99%.

Synovial tissues and treatments

Synovial tissues were obtained from patients with active RA, diagnosed according to the criteria of the American College of Rheumatology (formerly the American Rheumatism Association) (42), undergoing joint replacement or synovectomy. This study was approved by the Human Subjects Research Committee of our university. Informed consent was obtained from all subjects enrolled in the study. Synovial membrane samples were perfused with 5% glutaraldehyde, and paraffin sections (3 μm thick) were prepared for immunohistochemical studies. Synovial membrane and cartilage were also dissected under sterile conditions in PBS and immediately prepared for coimplantation to SCID mice.

Cell cultures

Synovial tissues samples were dissected under sterile conditions in PBS and immediately prepared for culture of fibroblast-like synovial cells. In brief, the tissue sample was minced into small pieces and digested with collagenase (Sigma Aldrich Japan, Tokyo) in serum-free DMEM (Life Technologies BRL, Grand Island, NY). After filtering through a nylon mesh, the cells were extensively washed and suspended in DMEM, supplemented with 10% FCS (Bio-Pro, Karlsruhe, Germany). Finally, isolated cells were seeded in 25-cm^2 culture flasks (Falcon, Lincoln Park, NJ) and cultured in a humidified 5% carbon dioxide atmosphere. After overnight culture, nonadherent cells were removed and incubation of adherent cells was continued in a fresh medium. At confluence, the cells were trypsinized, passaged at a 1:3 split ratio, and recultured. The medium was changed twice each week, and the cells were used after three to five passages.

Quantitative analysis of IFN-γ, IL-5, IL-17, IL-1β, TGF-β1, and IL-6

Cytokine concentrations in culture supernatant were measured by ELISA kit (R&D Systems).

Quantitative real-time PCR

Total RNA was extracted using the RNeasy mini kit (Qiagen, Tokyo, Japan), according to the manufacturer's instructions. cDNA was reverse transcribed using the high-capacity RNA-to-cDNA Master Mix (Applied Biosystems, Tokyo, Japan). Primers and probes were all predesigned TaqMan Gene Expression Assays from Applied Biosystems. Real-time PCR was performed on the StepOnePlus Real-Time PCR System (Applied Biosystems) machine. Predeveloped specific primers were used to detect *rorc* (Hs01076112) and 18s (Hs99999901). Target gene expression was normalized using 18s expression level and expressed in arbitrary units.

Cell viability assay

Cell viability was assessed using a TetraColor One kit including WST-8 [2-(2-methoxy-4-nitrophenyl)-3-(4-nitrophenyl)-5-(2,4-disulfophenyl)-2H-tetrazolium] and electron carrier mixture (Seikagaku, Tokyo, Japan). The WST-8 assay is based on the conversion of tetrazolium salt WST-8 to the highly water-soluble formazan. Cells (1×10^5) were seeded and incubated on a 96-well flat-bottom plate (Iwaki) in DMEM containing 10% FCS in a final volume of 0.1 ml for 24 h at 37°C. They were treated with different agents for various time intervals. Ten milliliters of a solution containing 5 mM WST-8, 0.2 mM 1-methoxy-5-methylphenazium methosulfate, and 150 mM NaCl was added to each well. After incubation for 2 h at 37°C, the OD of each well was measured on a microplate reader at 450 nm.

Flow cytometric detection of cell-surface dopamine receptors

Staining and flow cytometric analysis of synovial fibroblasts were carried out by standard procedures as already described using a FACSCalibur (BD Biosciences). Anti-dopamine D1–D5 receptor rabbit polyclonal Abs were obtained from Calbiochem. In brief, synovial fibroblasts (1×10^5 cells/sample) were incubated with anti-dopamine receptor polyclonal Ab for 20 min at 4°C, followed by FITC-conjugated anti-rabbit IgG (Sigma) at saturating concentrations in FACS medium consisting of HBSS (Nissui, Tokyo, Japan), 0.5% human serum albumin (Mitsubishi Pharma, Osaka,

Japan), and 0.2% NaN_3 (Sigma) for 20 min at 4°C. After three washes in FACS medium, the cells were analyzed with the FACSCalibur.

Fractional catecholamine analysis

Ten patients with RA and 10 control patients with osteoarthritis (OA) were diagnosed according to the American College of Rheumatology criteria (42). Synovial fluid specimens were collected during either diagnostic or therapeutic arthrocentesis of the knee (10 knees in 10 cases with RA and 10 knees in 10 cases with OA; Table I). All synovial samples were collected under sterile conditions, and the cellular components were removed immediately after centrifugation. The supernatants were stored at −30°C. The supernatants were transferred immediately to a test tube containing perchloric acid (final concentration, 0.4 M). Catecholamines (dopamine, noradrenaline, and adrenaline) were adsorbed onto aluminum hydroxide and estimated by the ethylenediamine condensation method using a fluorescence spectrophotometer (F-4010; Hitachi, Tokyo, Japan) with excitation and emission wavelengths of 420 and 540 nm, respectively (43).

Preparation of human RA/SCID chimera mice and treatment with dopamine receptor antagonists

Human RA/SCID chimera mice were evaluated as models for the treatment study. A total of 18 male SCID mice (CR.17/lcr; CLEA Japan, Tokyo, Japan), 6- to 7-wk-old, which had been bred under specific pathogen-free conditions at our university animal center, were used for establishment of the human RA/SCID chimera mouse model. Pannus tissue from synovial membrane, cartilage, and bone, collected as a mass from RA patients at the time of surgery, was used for implantation. The size of the removed specimen was adjusted to a block almost 4–8 mm in diameter before implantation. The mice were anesthetized with diethyl ether, according to the guidelines established by the animal ethics committee of the University of Occupational and Environmental Health, Japan. The tissue implants were grafted s.c. on the backs of the mice. All surgical procedures were performed under sterile conditions. The mice were randomly assigned to three groups at 1 wk after the implantation. The mice in the test groups were s.c. administered 0.3 mg/kg haloperidol (a D2-like receptor antagonist; Sigma, Japan) or 0.3 mg/kg SCH-23390 (a D1-like receptor antagonist; Sigma) twice a week for 3 wk. The mice in the control group received 50 μl PBS. Thirty days after implantation, the mice were anesthetized and their implanted tissues were removed. The animal experiments were approved by and performed in compliance with the guidelines of the Institutional Animal Care and Use Committee.

Histochemical analysis

The 3-μm-thick sections prepared from RA synovial tissues were incubated with rabbit anti-dopamine Ab (Chemicon) or S-100 and then incubated with secondary Ab (EnVision+; Dako) (44, 45). The implanted tissues were removed and histologically observed after H&E staining. To examine biological activities of the implanted tissues, we performed immunohistochemical staining as previously described (44, 45). The sections were stained with the following anti-human monoclonal Abs and an immunostaining kit: IFN-γ, IL-17, IL-6, and EnVision+. These were purchased from Dako Japan.

Statistical analysis

Parametric testing among three or more groups was performed by ANOVA. Nonparametric testing was performed using the Mann–Whitney rank sum test.

Results

Dopamine increases IL-6–dependent IL-17 secretion from human T cells

We have previously reported that only D1 was specifically expressed at a high level in $CD4^+$ naive T cells, and that dopamine increased the cAMP concentrations in $CD4^+$ naive T cells via D1-like receptors, and subsequently induced the secretion of IL-4 and IL-5 (19, 41). In this study, we first examined the pattern of cytokine secretion including IL-17 from $CD4^+$ naive T cells, which were stimulated by anti-CD3/CD28 Abs and simultaneously added dopamine. Dopamine slightly increased IL-5 secretion without affecting IFN-γ production, whereas dopamine markedly increased IL-17 secretion in a dose-dependent manner, indicating dopamine as an important factor for Th17 differentiation rather than Th2 differentiation (Fig. 1*A*). We also measured the concentration of Th17-inducible cytokines such as IL-6, IL-1β, and TGF-β. Interestingly, IL-6 secretion also increased in a dose-dependent manner (Fig. 1*B*), whereas minimum IL-1β and no TGF-β secretion were observed (data not shown). At the same time, we investigated the response of naive human T cells to

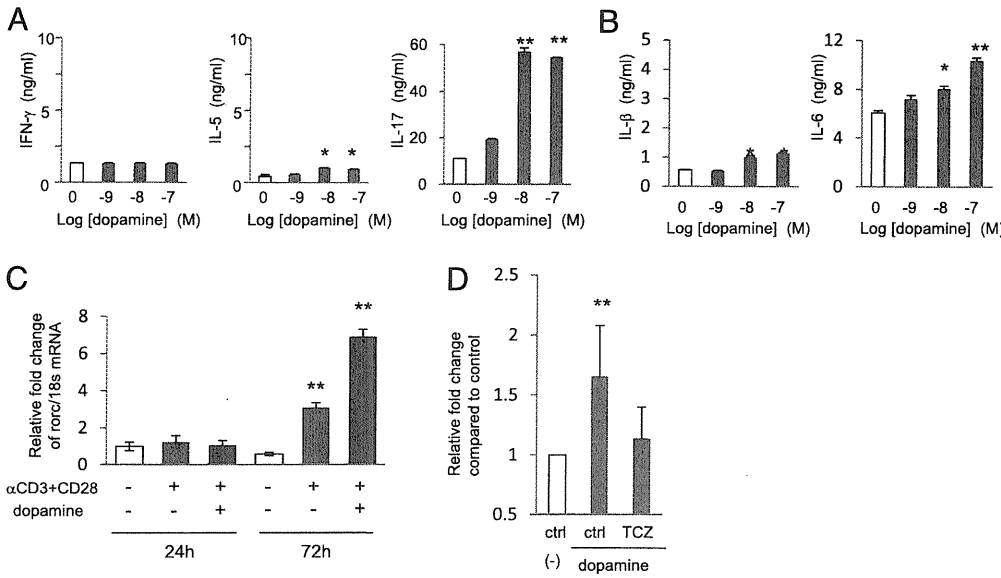

FIGURE 1. Dopamine-mediated cytokine secretion from $CD4^+$ T cells. Purified human $CD4^+$ naive T cells were stimulated with anti-CD3 and anti-CD28 plate-bound Abs, and with the indicated concentrations of dopamine. *A*, ELISA for IFN-γ, IL-5, and IL-17 was performed on the supernatants after a 3-d culture period. *B*, Cytokine beads array for IL-1β and IL-6 was performed on the supernatants after a 3-d culture period. *C*, Real-time PCR analysis of the expression of *rorc* transcript after stimulation. mRNA values were normalized to 18s. Purified human $CD4^+$ naive T cells were pretreated with 200 μg/ml tocilizumab or γ-globulin (as a control Ab) for 30 min and stimulated with 50 ng/ml PMA and 1 μg/ml ionomycin (*D*). PBS served as a negative control. Data are mean ± SD of five experiments in triplicate. Statistically significant differences are indicated by asterisks. $^{**}p < 0.01$, $^{*}p < 0.05$ versus control. Figures represent three independent experiments.

dopamine without anti-CD3/CD28 Abs. However, all cytokines that we tested were undetectable or very low level (data not shown). Furthermore, we investigated the *rorc* mRNA expression in these cells after stimulation with dopamine by quantitative PCR (Fig. 1*C*). Stimulation with anti-CD3/CD28 Abs induced the *rorc* mRNA expression, whereas dopamine markedly increased the expression level at 72 h. The induction of IL-17 secretion, which was dopamine dependent, was almost completely inhibited when human $CD4^+$ naive T cells were pretreated with tocilizumab, an anti-human IL-6R Ab (Fig. 1*D*). These results suggested that dopamine increases IL-17 production from T cells via IL-6 production.

D1-like receptor antagonists inhibit dopamine-mediated IL-6 and IL-17 secretion from human T cells

The IL-6 gene promoter contains a cAMP response element (46). In our previous studies, we showed that dopamine-mediated cAMP elevation in human $CD4^+$ naive T cells was completely inhibited by treatment with SCH-23390, a selective D1-like antagonist (41). To evaluate whether antagonizing D1-like receptors decreases dopamine-mediated IL-6 and IL-17 production, we treated $CD4^+$ naive T cells with or without SCH-23390, and then IL-6 and IL-17 secretion was determined by ELISA. As shown in Fig. 2, SCH-23390 completely inhibited dopamine-mediated IL-6 and IL-17 secretion from T cells. This inhibitory effect by antagonizing D1-like receptors was demonstrated not only by SCH-23390, but by LE300, another D1-like receptor antagonist (data not shown), indicating that antagonizing D1-like receptor inhibited dopamine-mediated IL-6–Th17 axis.

Dopamine is detected in inflamed synovial tissue in RA

To investigate the roles of dopamine in the pathogenesis of synovitis in RA, we measured catecholamine concentrations in synovial fluid of RA and OA patients (Table I). Although it is necessary to compare RA synovial tissue with synovial tissue from healthy individuals, we could not obtain samples from healthy individuals. Concentrations of noradrenalin and adrenaline did not differ between RA and OA patients, but dopamine was significantly higher in RA patients (Fig. 3*A*). Presumably, dopamine-producing cells were increased at the site of synovitis in RA. In the synovial tissues from RA patients, S100-positive DCs were also stained with dopamine, and an accumulation of lymphocytes

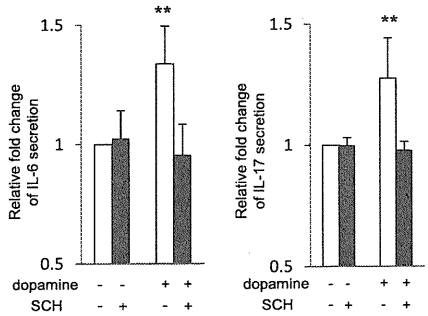

FIGURE 2. Suppression of dopamine-mediated upregulation of IL-6 and IL-17 production by a D1-like dopamine receptor antagonist. Purified human $CD4^+$ naive T cells were stimulated with anti-CD3 and anti-CD28 plate-bound Abs, 1 μM dopamine, and with or without 10 μM SCH-23390. White and gray bars represent without and with SCH-23390 exposure, respectively. Results are shown as relative fold changes compared with control cytokine production (not exposed to dopamine and SCH-23390). Data are mean ± SD of five experiments in triplicate. Statistically significant differences are indicated by asterisks. $^{**}p < 0.01$ versus control.

Table I. Clinical features of the participants who contributed synovial fluid

Characteristics	RA	OA
No. of participants	10	10
Sex, male/female	1/9	2/8
Mean age, y (range)	65.2 (39–85)	69.5 (57–78)
Mean disease duration, y (range)	5.2 (0.6–15)	NA
Mean CRP, mg/dl (range)	2.8 (1.5–4.4)	NA
Mean MMP3, ng/ml (range)	441.6 (135–738)	NA

CRP, C-reactive protein; MMP3, matrix metalloproteinase-3; NA, not applicable.

was prominently observed in the surroundings of DCs (Fig. 3*B*, 3*C*). Thus, it seems likely that there are DCs that synthesized and stored dopamine in RA synovial tissue.

Dopamine receptor antagonists on rheumatoid synovitis in SCID mice engrafted with human RA synovium mice

Next, to evaluate the relevance of these findings in vivo, we studied the effect of dopamine receptor antagonists in a model of the SCID mouse in which active RA synovial tissue and cartilage have been engrafted (SCID mice engrafted with human RA synovium [SCID-HuRAg]) (47). SCID-HuRAg mice were divided into three groups ($n = 6$) 1 wk after the transplantation, and an antagonist of D1-like receptors (SCH-23390), an antagonist of D2-like receptors (haloperidol), or vehicle (control) was administered twice a week for 3 wk for each group. The grafts were collected 30 d after implantation and pathological evaluation was performed. Macroscopically, remarkable retraction of synovial tissue was observed in the group that received D1-like receptor antagonist. In contrast, vascular proliferation and enlargement of tissue were observed in the group administered with D2-like receptor antagonist (Fig. 4*A*). The histopathological findings showed only slight

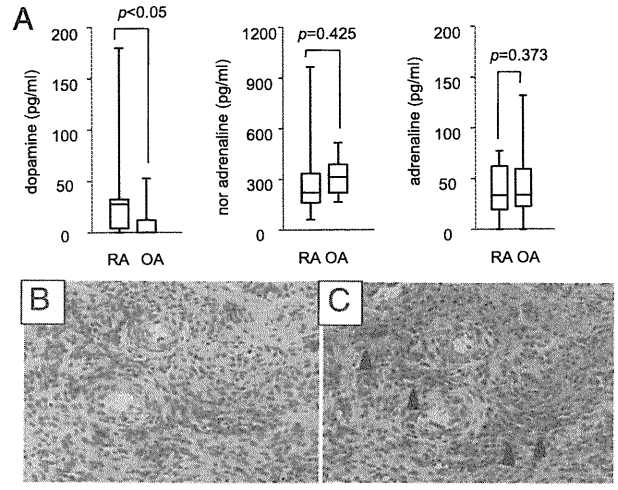

FIGURE 3. Presence of catecholamine in synovial fluids and the storage of dopamine in synovial tissue. *A*, Synovial fluids obtained from 10 patients with RA and 10 patients with OA were analyzed by HPLC electrochemical detection for dopamine, noradrenaline, and adrenaline. The composite results are presented as box plots, where the boxes represent the 25th to 75th percentiles, the lines within the boxes represent the median, and the lines outside the boxes represent the 10th to 90th percentiles. *B* and *C*, Immunohistochemical staining of S-100 protein (*B*) and dopamine (*C*) in RA synovial tissue (brown staining). Arrowheads indicate dopamine-stored cells (original magnification ×20). Sections are representative for three patients.

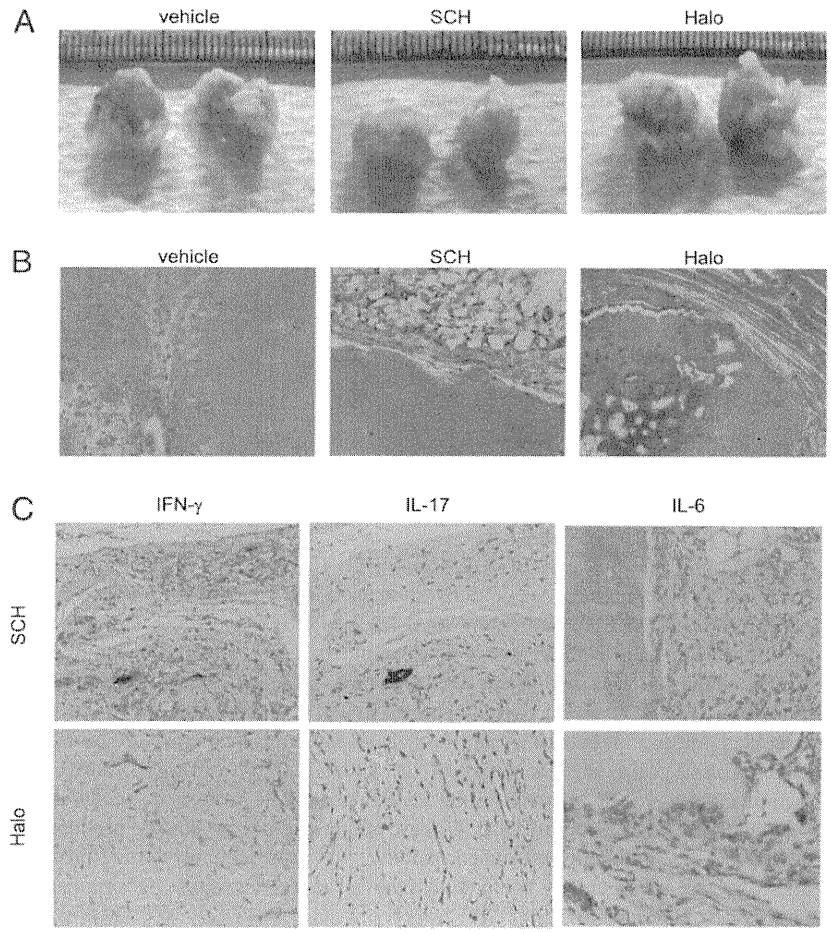

FIGURE 4. Differential effects of dopamine D1- and D2-like antagonists on experimental arthritis. *A*, The removed tissues containing synovium and cartilage from SCID-HuRAg mice. *B*, H&E-stained sections 30 d after implantation (original magnification ×20). *C*, IFN-γ and IL-6 are observed on brown staining. IL-17 is observed on pink staining. SCH23390-treated mice (*top panels*). Haloperidol-treated mice (*bottom panels*) (original magnification ×20). Sections are representative for $n \geq 3$ per group.

cartilage destruction, shrinkage of synovial fibroblasts, and prominent IFN-γ–producing cells in the group administered with D1-like receptor antagonist (Fig. 4*B*, 4*C*). In contrast, the group administered with D2-like receptor antagonist had marked cartilage destruction, synovial hyperplasia with angiogenesis, and prominent IL-6^+ and IL-17^+ cells (Fig. 4*B*, 4*C*). The effect of antagonizing D1-like receptor antagonist was demonstrated not only by SCH-23390, but by LE300, which is a selective D1-like receptor antagonist (data not shown).

D1-like receptor antagonists do not influence the viability of RA synovial fibroblasts

To clarify whether the retraction of synovial tissue in SCID-HuRAg mice treated with D1-like receptor antagonists is due to direct effect on synovial fibroblasts, we evaluated cell viability of SCH-23390–treated synovial fibroblasts using a WST-8 assay.

No significant differences were observed between antagonist-treated and untreated groups (Fig. 5*A*). Furthermore, we investigated the expression of dopamine receptors on synovial fibroblasts derived from RA patients. However, no D1–D5 subtype was detected on synovial fibroblasts (Fig. 5*B*). These results indicated that antagonizing D1-like receptors did not reduce synovial tissue in SCID-HuRAg mice directly.

Discussion

Dopamine has been shown to act on receptors present on immune cells, with all subtypes of dopamine receptors found on leukocytes (7, 8, 10). Interestingly, disorders such as schizophrenia and Parkinson's disease, in which there are changes in dopamine receptors and dopamine signaling pathways not only in brain, but in lymphocytes, are also associated with altered immune functioning (48). For example, in patients with schizophrenia thought to be

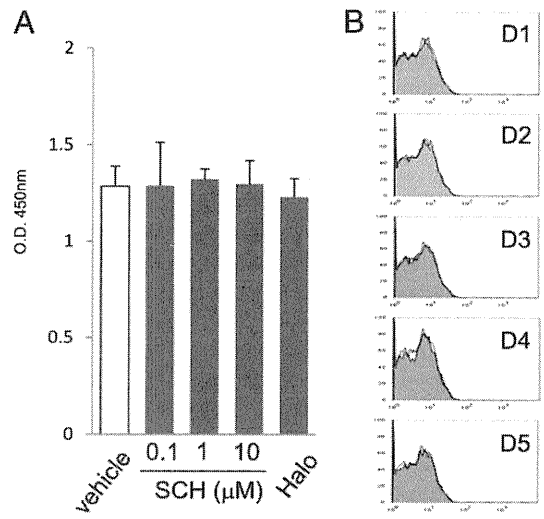

FIGURE 5. *A*, Effects of dopamine receptor antagonists on viability of synovial fibroblasts. Synovial fibroblasts were incubated with the indicated concentrations of SCH-23390 or 1 μM haloperidol for 24 h. Data are mean ± SD of five experiments in triplicate. *B*, The expression of dopamine receptor subtypes. The expression of dopamine receptor subtypes on human synovial fibroblasts was analyzed by a FACSCalibur. After fixation, cells were stained with Abs of indicated dopamine receptor subtypes and anti-rabbit IgG-FITC. Filled histograms indicate dopamine receptor subtypes; open histograms indicate isotype-matched control IgG. The results are representative of three experiments.

dependent on excessive response of D2-like dopamine receptors (49), the median incidence rate of RA is ~0.09% (50). This incidence is only one tenth that of RA in the general population, suggesting the involvement of dopamine signaling pathway in the pathogenesis of RA. However, there was no clear explanation for this epidemiological phenomenon.

The secondary lymphoid tissues are highly innervated by sympathetic nerve fibers that store high levels of dopamine (51), and lymphocytes also produce dopamine (52, 53). However, although RA synovium has been known to have the characteristics of lymphoid organs with regard to cellular composition and organization, a drastic loss of sympathetic nerve fibers in the RA synovium has been demonstrated (54). In our previous study, we demonstrated that monocyte-derived DC released vesicles containing dopamine toward T cells during DC–T cell interaction (41). Furthermore, we could detect dopamine only in DCs in RA synovium in our current study. These findings suggested that DC-derived dopamine during naive T cell–DC interaction may contribute to the development of RA.

During the development of RA, $CD45RA^+$ T cells may be attracted by chemokines secreted by tissue macrophages/DCs. Naive $CD45RA^+$ T cells expressing ICAM-3, which is a specific ligand of DC-specific ICAM-3–grabbing nonintegrin (DC-SIGN), are abundantly present within the RA synovium (55), suggesting that naive T cell–DC interaction is involved in cell activation and increased release of cytokines and enzymes. Although we had tried to characterize the phenotype of the putative DCs storing significant amounts of dopamine using several Abs to DC markers such as CD1a, CD123, and BDCA-2, these DC markers were not detectable by immunohistochemical staining, which is probably due to reduced antigenicity by fixation synovial membrane samples by 5% glutaraldehyde.

Although the concentration of dopamine in the RA synovial fluid was 0.1–10 nM, calculated dopamine concentration within 1 ms after unitary synaptic release was 100–250 nM within 1 μm in dopaminergic neurons (1). Because the space at DC–T cell synapses is within 1 μm (41), the concentration of dopamine in the synapse is estimated to be 100–250 nM, thus indicating that $CD4^+$ naive T cells might be exposed to a relatively high concentration of dopamine during DC–T cell interaction. The concentration of the dopamine we used was high compared with previous reports. However, when naive CD4 T cells were stimulated with both anti-CD3/CD28 mAb and dopamine, cell viability was not affected by dopamine up to 10 μM (data not shown). Previous in vitro studies testing dopamine at relatively high concentrations demonstrated that dopamine was immunosuppressive (14, 15). In contrast, in vivo administration of pharmacological doses of dopamine was reported to be mostly immunostimulatory (56). Thus, dopamine could be either immunostimulatory or immunosuppressive depending on the experimental condition used. However, it is highly possible that these findings are dependent on the expression pattern and the level of dopamine receptors.

Studies carried out on human and murine T cells have demonstrated that these cells express all subtypes of dopamine receptors, each of which has diverse modulatory effects on the T cell physiology. D1- and D2-like dopamine receptors are coupled to stimulation and inhibition of intracellular cAMP production, respectively (2, 13). Stimulation of the D1-like receptor impairs T cell function by increasing intracellular cAMP levels. Stimulation of D1-like receptor not only inhibits cytotoxic function of $CD8^+$ T cells (57), but impairs function and differentiation of regulatory T cells (Tregs) (53, 58). Stimulation of dopamine D2-like receptors in normal resting peripheral human T lymphocytes induces integrin-mediated adhesion to fibronectin (4) and increases the secretion of TNF-α (primarily via D3 receptors) and the secretion of IL-10 (primarily via D2 receptors) without affecting the secretion of IFN-γ and IL-4 (7). However, because these normal resting peripheral human T lymphocytes were not purified, they were different in quality from $CD4^+CD45RA^+$ naive T cells, which we used in this study. We have already reported that there were differences in the expression pattern of dopamine receptor subtypes between naive CD4 T cells and memory CD4 T cells (19), and that dopamine increases intracellular cAMP levels in naive CD4 T cells but decreases them in memory CD4 T cells (41). Therefore, high purity of $CD4^+CD45RA^+$ naive T cells was needed to reproduce the series of our results.

We have previously demonstrated that D1-like receptors were functionally dominant, and that dopamine increased cAMP levels via D1-like receptors and induced the production of Th2 cytokine such as IL-4 and IL-5, in response to anti-CD3/CD28 mAb (41). Regarding regulation of TCR-triggered signaling by cAMP in T cells, protein kinase A (a protein kinase activated by cAMP) and cAMP induce inhibition of ERK phosphorylation (59) and of JNK activation (60), activate C-terminal Src kinase (61), and block NF-κB activation (62, 63). All of these intracellular biochemical events induce a marked impairment on T cell activation with inhibition of T cell proliferation and of cytokine production (64). In this study, we showed that dopamine markedly increased IL-17 production from T cells via IL-6 production, in response to anti-CD3/CD28 mAb. Because the IL-6 gene promoter contains a cAMP response element (46), it is likely that increased intracellular cAMP via D1-like receptors of T cells induces IL-6 production, which act as autocrine or paracrine stimulus for IL-17 production in short-term culture. Although murine Th17 cells originate from $CD4^+$ naive T cells in the presence of IL-6 and TGF-β, the precise conditions for human Th17 differentiation remain controversial (65). Therefore, further studies are needed to elucidate the potential role of dopamine in human Th17 differentiation by long-term culture in the presence of TGF-β. However, in a human RA/SCID mouse chimera model, antagonizing dopamine receptor subtypes differentially affected cytokine expression, indicating that dopamine produced by DCs that accumulated in synovial tissue of RA established a Th17-predominant immune system via IL-6 and IL-17 production from T cells, leading to aggravation of synovitis and cartilage destruction.

Interestingly, it has been reported that dopamine reduces the suppressive and trafficking activities of naturally occurring Treg through D1-like receptors in both human and mouse (53, 58), and that dopamine-mediated downregulation of naturally occurring Tregs was selectively reversed by treatment with SCH-23390 (53, 58), indicating that DC-derived dopamine causes prolongation of RA synovitis via inhibition of Treg, as well as IL-6–Th17 bias. In other words, application of a D1-like receptor antagonist can be expected to control autoimmune disorders such as RA via two mechanisms: inhibition of IL-6–Th17 bias and increase in Treg activity. Actually, D1-like receptor antagonists exhibited preventive and therapeutic effects on model mice of autoimmune diseases such as EAE in mice, diabetes mellitus that occurs naturally in NOD mice, and crescent formation in nephrotoxic serum nephritis mice (19, 66, 67).

In this study, the specific importance of neuroimmune cross talk during pathological processes of various immune-inflammatory diseases was indicated, to our knowledge, for the first time by the discovery of dopamine production in DCs, which are the immunological sentinels at the front line of tissue defense and subsequent induction of Th17-predominant immune disease. In addition, approach from a different perspective could lead to new treatment applications of these findings.

Acknowledgments

We thank N. Sakaguchi, K. Noda, T. Adachi, and S. Shinohara for technical assistance.

Disclosures

Y.T. has received consulting fees, speaking fees, and/or honoraria from Mitsubishi Tanabe Pharma; Chugai Pharmaceutical Co., Ltd.; Eisai Co., Ltd.; Takeda Pharmaceutical Co., Ltd.; and Abbott Japan and has received research grant support from Mitsubishi Tanabe Pharma; Takeda Pharmaceutical Co., Ltd.; MSD; Pfizer; Astellas Pharma; Chugai Pharmaceutical Co., Ltd.; Abbott Japan; and Eisai Co., Ltd.

References

1. Wickens, J. R., and G. W. Arbuthnott. 2005. Structural and functional interactions in the striatum at the receptor level. In *Handbook of Chemical Neuroanatomy.* S. B. Dunnet, M. Bentivoglio, A. Bjorklund, and T. Hokfelt, eds. Elsevier Science Publishing Co., Amsterdam, p. 199–236.
2. Missale, C., S. R. Nash, S. W. Robinson, M. Jaber, and M. G. Caron. 1998. Dopamine receptors: from structure to function. *Physiol. Rev.* 78: 189–225.
3. Ganor, Y., M. Besser, N. Ben-Zakay, T. Unger, and M. Levite. 2003. Human T cells express a functional ionotropic glutamate receptor GluR3, and glutamate by itself triggers integrin-mediated adhesion to laminin and fibronectin and chemotactic migration. *J. Immunol.* 170: 4362–4372.
4. Levite, M., Y. Chowers, Y. Ganor, M. Besser, R. Hershkovits, and L. Cahalon. 2001. Dopamine interacts directly with its D3 and D2 receptors on normal human T cells, and activates beta1 integrin function. *Eur. J. Immunol.* 31: 3504–3512.
5. Franco, R., R. Pacheco, C. Lluis, G. P. Ahern, and P. J. O'Connell. 2007. The emergence of neurotransmitters as immune modulators. *Trends Immunol.* 28: 400–407.
6. Pacheco, R., H. Oliva, J. M. Martinez-Navío, N. Climent, F. Ciruela, J. M. Gatell, T. Gallart, J. Mallol, C. Lluis, and R. Franco. 2006. Glutamate released by dendritic cells as a novel modulator of T cell activation. *J. Immunol.* 177: 6695–6704.
7. Besser, M. J., Y. Ganor, and M. Levite. 2005. Dopamine by itself activates either D2, D3 or D1/D5 dopaminergic receptors in normal human T-cells and triggers the selective secretion of either IL-10, TNFalpha or both. *J. Neuroimmunol.* 169: 161–171.
8. Saha, B., A. C. Mondal, S. Basu, and P. S. Dasgupta. 2001. Circulating dopamine level, in lung carcinoma patients, inhibits proliferation and cytotoxicity of CD4+ and CD8+ T cells by D1 dopamine receptors: an in vitro analysis. *Int. Immunopharmacol.* 1: 1363–1374.
9. Sarkar, C., S. Das, D. Chakroborty, U. R. Chowdhury, B. Basu, P. S. Dasgupta, and S. Basu. 2006. Cutting edge: stimulation of dopamine D4 receptors induce T cell quiescence by up-regulating Kruppel-like factor-2 expression through inhibition of ERK1/ERK2 phosphorylation. *J. Immunol.* 177: 7525–7529.
10. Watanabe, Y., T. Nakayama, D. Nagakubo, K. Hieshima, Z. Jin, F. Katou, K. Hashimoto, and O. Yoshie. 2006. Dopamine selectively induces migration and homing of naive CD8+ T cells via dopamine receptor D3. *J. Immunol.* 176: 848–856.
11. O'Connell, P. J., X. Wang, M. Leon-Ponte, C. Griffiths, S. C. Pingle, and G. P. Ahern. 2006. A novel form of immune signaling revealed by transmission of the inflammatory mediator serotonin between dendritic cells and T cells. *Blood* 107: 1010–1017.
12. Kawashima, K., and T. Fujii. 2003. The lymphocytic cholinergic system and its contribution to the regulation of immune activity. *Life Sci.* 74: 675–696.
13. Sibley, D. R., F. J. Monsma, Jr., and Y. Shen. 1993. Molecular neurobiology of dopaminergic receptors. *Int. Rev. Neurobiol.* 35: 391–415.
14. Ghosh, M. C., A. C. Mondal, S. Basu, S. Banerjee, J. Majumder, D. Bhattacharya, and P. S. Dasgupta. 2003. Dopamine inhibits cytokine release and expression of tyrosine kinases, Lck and Fyn in activated T cells. *Int. Immunopharmacol.* 3: 1019–1026.
15. Bergquist, J., E. Josefsson, A. Tarkowski, R. Ekman, and A. Ewing. 1997. Measurements of catecholamine-mediated apoptosis of immunocompetent cells by capillary electrophoresis. *Electrophoresis* 18: 1760–1766.
16. Takahashi, N., Y. Nagai, S. Ueno, Y. Saeki, and T. Yanagihara. 1992. Human peripheral blood lymphocytes express D5 dopamine receptor gene and transcribe the two pseudogenes. *FEBS Lett.* 314: 23–25.
17. Ricci, A., E. Bronzetti, F. Mignini, S. K. Tayebati, D. Zaccheo, and F. Amenta. 1999. Dopamine D1-like receptor subtypes in human peripheral blood lymphocytes. *J. Neuroimmunol.* 96: 234–240.
18. McKenna, F., P. J. McLaughlin, B. J. Lewis, G. C. Sibbring, J. A. Cummerson, D. Bowen-Jones, and R. J. Moots. 2002. Dopamine receptor expression on human T- and B-lymphocytes, monocytes, neutrophils, eosinophils and NK cells: a flow cytometric study. *J. Neuroimmunol.* 132: 34–40.
19. Nakano, K., T. Higashi, K. Hashimoto, R. Takagi, Y. Tanaka, and S. Matsushita. 2008. Antagonizing dopamine D1-like receptor inhibits Th17 cell differentiation: preventive and therapeutic effects on experimental autoimmune encephalomyelitis. *Biochem. Biophys. Res. Commun.* 373: 286–291.
20. Volpe, E., N. Servant, R. Zollinger, S. I. Bogiatzi, P. Hupé, E. Barillot, and V. Soumelis. 2008. A critical function for transforming growth factor-beta, interleukin 23 and proinflammatory cytokines in driving and modulating human T (H)-17 responses. *Nat. Immunol.* 9: 650–657.
21. Yang, L., D. E. Anderson, C. Baecher-Allan, W. D. Hastings, E. Bettelli, M. Oukka, V. K. Kuchroo, and D. A. Hafler. 2008. IL-21 and TGF-β are required for differentiation of human T(H)17 cells. *Nature* 454: 350–352.
22. Santarlasci, V., L. Maggi, M. Capone, F. Frosali, V. Querci, R. De Palma, F. Liotta, L. Cosmi, E. Maggi, S. Romagnani, and F. Annunziato. 2009. TGF-β indirectly favors the development of human Th17 cells by inhibiting Th1 cells. *Eur. J. Immunol.* 39: 207–215.
23. Cua, D. J., J. Sherlock, Y. Chen, C. A. Murphy, B. Joyce, B. Seymour, L. Lucian, W. To, S. Kwan, T. Churakova, et al. 2003. Interleukin-23 rather than interleukin-12 is the critical cytokine for autoimmune inflammation of the brain. *Nature* 421: 744–748.
24. Murphy, C. A., C. L. Langrish, Y. Chen, W. Blumenschein, T. McClanahan, R. A. Kastelein, J. D. Sedgwick, and D. J. Cua. 2003. Divergent pro- and antiinflammatory roles for IL-23 and IL-12 in joint autoimmune inflammation. *J. Exp. Med.* 198: 1951–1957.
25. Kotake, S., N. Udagawa, N. Takahashi, K. Matsuzaki, K. Itoh, S. Ishiyama, S. Saito, K. Inoue, N. Kamatani, M. T. Gillespie, et al. 1999. IL-17 in synovial fluids from patients with rheumatoid arthritis is a potent stimulator of osteoclastogenesis. *J. Clin. Invest.* 103: 1345–1352.
26. Chabaud, M., J. M. Durand, N. Buchs, F. Fossiez, G. Page, L. Frappart, and P. Miossec. 1999. Human interleukin-17: a T cell-derived proinflammatory cytokine produced by the rheumatoid synovium. *Arthritis Rheum.* 42: 963–970.
27. Ziolkowska, M., A. Koc, G. Luszczykiewicz, K. Ksiezopolska-Pietrzak, E. Klimczak, H. Chwalinska-Sadowska, and W. Maslinski. 2000. High levels of IL-17 in rheumatoid arthritis patients: IL-15 triggers in vitro IL-17 production via cyclosporin A-sensitive mechanism. *J. Immunol.* 164: 2832–2838.
28. Honorati, M. C., R. Meliconi, L. Pulsatelli, S. Canè, L. Frizziero, and A. Facchini. 2001. High in vivo expression of interleukin-17 receptor in synovial endothelial cells and chondrocytes from arthritis patients. *Rheumatology (Oxford)* 40: 522–527.
29. Kirkham, B. W., M. N. Lassere, J. P. Edmonds, K. M. Juhasz, P. A. Bird, C. S. Lee, R. Shnier, and I. J. Portek. 2006. Synovial membrane cytokine expression is predictive of joint damage progression in rheumatoid arthritis: a two-year prospective study (the DAMAGE study cohort). *Arthritis Rheum.* 54: 1122–1131.
30. Chabaud, M., F. Fossiez, J.-L. Taupin, and P. Miossec. 1998. Enhancing effect of IL-17 on IL-1-induced IL-6 and leukemia inhibitory factor production by rheumatoid arthritis synoviocytes and its regulation by Th2 cytokines. *J. Immunol.* 161: 409–414.
31. Chabaud, M., G. Page, and P. Miossec. 2001. Enhancing effect of IL-1, IL-17, and TNF-α on macrophage inflammatory protein-3α production in rheumatoid arthritis: regulation by soluble receptors and Th2 cytokines. *J. Immunol.* 167: 6015–6020.
32. Katz, Y., O. Nadiv, and Y. Beer. 2001. Interleukin-17 enhances tumor necrosis factor alpha-induced synthesis of interleukins 1,6, and 8 in skin and synovial fibroblasts: a possible role as a "fine-tuning cytokine" in inflammation processes. *Arthritis Rheum.* 44: 2176–2184.
33. Lundy, S. K., S. Sarkar, L. A. Tesmer, and D. A. Fox. 2007. Cells of the synovium in rheumatoid arthritis. T lymphocytes. *Arthritis Res. Ther.* 9: 202.
34. Gaffen, S. L. 2004. Biology of recently discovered cytokines: interleukin-17—a unique inflammatory cytokine with roles in bone biology and arthritis. *Arthritis Res. Ther.* 6: 240–247.
35. Miranda-Carús, M. E., M. Benito-Miguel, A. Balsa, T. Cobo-Ibáñez, C. Pérez de Ayala, D. Pascual-Salcedo, and E. Martín-Mola. 2006. Peripheral blood T lymphocytes from patients with early rheumatoid arthritis express RANKL and interleukin-15 on the cell surface and promote osteoclastogenesis in autologous monocytes. *Arthritis Rheum.* 54: 1151–1164.
36. Sato, K., A. Suematsu, K. Okamoto, A. Yamaguchi, Y. Morishita, Y. Kadono, S. Tanaka, T. Kodama, S. Akira, Y. Iwakura, et al. 2006. Th17 functions as an osteoclastogenic helper T cell subset that links T cell activation and bone destruction. *J. Exp. Med.* 203: 2673–2682.
37. Koenders, M. I., E. Lubberts, F. A. J. van de Loo, B. Oppers-Walgreen, L. van den Bersselaar, M. M. Helsen, J. K. Kolls, F. E. Di Padova, L. A. B. Joosten, and W. B. van den Berg. 2006. Interleukin-17 acts independently of TNF-α under arthritic conditions. *J. Immunol.* 176: 6262–6269.
38. Koenders, M. I., J. K. Kolls, B. Oppers-Walgreen, L. van den Bersselaar, L. A. B. Joosten, J. R. Schurr, P. Schwarzenberger, W. B. van den Berg, and E. Lubberts. 2005. Interleukin-17 receptor deficiency results in impaired synovial expression of interleukin-1 and matrix metalloproteinases 3, 9, and 13 and prevents cartilage destruction during chronic reactivated streptococcal cell wall-induced arthritis. *Arthritis Rheum.* 52: 3239–3247.
39. Genovese, M. C., F. Van den Bosch, S. A. Roberson, S. Bojin, I. M. Biagini, P. Ryan, and J. Sloan-Lancaster. 2010. LY2439821, a humanized anti-interleukin-17 monoclonal antibody, in the treatment of patients with rheumatoid arthritis: a phase I randomized, double-blind, placebo-controlled, proof-of-concept study. *Arthritis Rheum.* 62: 929–939.
40. Murphy, K. M., W. Ouyang, J. D. Farrar, J. Yang, S. Ranganath, H. Asnagli, M. Afkarian, and T. L. Murphy. 2000. Signaling and transcription in T helper development. *Annu. Rev. Immunol.* 18: 451–494.
41. Nakano, K., T. Higashi, R. Takagi, K. Hashimoto, Y. Tanaka, and S. Matsushita. 2009. Dopamine released by dendritic cells polarizes Th2 differentiation. *Int. Immunol.* 21: 645–654.
42. Arnett, F. C., S. M. Edworthy, D. A. Bloch, D. J. McShane, J. F. Fries, N. S. Cooper, L. A. Healey, S. R. Kaplan, M. H. Liang, H. S. Luthra, et al. 1988.

The American Rheumatism Association 1987 revised criteria for the classification of rheumatoid arthritis. *Arthritis Rheum.* 31: 315–324.
43. Yanagihara, N., Y. Oishi, H. Yamamoto, M. Tsutsui, J. Kondoh, T. Sugiura, E. Miyamoto, and F. Izumi. 1996. Phosphorylation of chromogranin A and catecholamine secretion stimulated by elevation of intracellular Ca2+ in cultured bovine adrenal medullary cells. *J. Biol. Chem.* 271: 17463–17468.
44. Sasaguri, Y., K.-Y. Wang, A. Tanimoto, M. Tsutsui, H. Ueno, Y. Murata, Y. Kohno, S. Yamada, and H. Ohtsu. 2005. Role of histamine produced by bone marrow-derived vascular cells in pathogenesis of atherosclerosis. *Circ. Res.* 96: 974–981.
45. Nakano, K., Y. Okada, K. Saito, R. Tanikawa, N. Sawamukai, Y. Sasaguri, T. Kohro, Y. Wada, T. Kodama, and Y. Tanaka. 2007. Rheumatoid synovial endothelial cells produce macrophage colony-stimulating factor leading to osteoclastogenesis in rheumatoid arthritis. *Rheumatology (Oxford)* 46: 597–603.
46. Sitaraman, S. V., D. Merlin, L. Wang, M. Wong, A. T. Gewirtz, M. Si-Tahar, and J. L. Madara. 2001. Neutrophil-epithelial crosstalk at the intestinal lumenal surface mediated by reciprocal secretion of adenosine and IL-6. *J. Clin. Invest.* 107: 861–869.
47. Geiler, T., J. Kriegsmann, G. M. Keyszer, R. E. Gay, and S. Gay. 1994. A new model for rheumatoid arthritis generated by engraftment of rheumatoid synovial tissue and normal human cartilage into SCID mice. *Arthritis Rheum.* 37: 1664–1671.
48. Sarkar, C., B. Basu, D. Chakroborty, P. S. Dasgupta, and S. Basu. 2010. The immunoregulatory role of dopamine: an update. *Brain Behav. Immun.* 24: 525–528.
49. Abi-Dargham, A., J. Rodenhiser, D. Printz, Y. Zea-Ponce, R. Gil, L. S. Kegeles, R. Weiss, T. B. Cooper, J. J. Mann, R. L. Van Heertum, et al. 2000. Increased baseline occupancy of D2 receptors by dopamine in schizophrenia. *Proc. Natl. Acad. Sci. USA* 97: 8104–8109.
50. Oken, R. J., and M. Schulzer. 1999. At issue: schizophrenia and rheumatoid arthritis: the negative association revisited. *Schizophr. Bull.* 25: 625–638.
51. Weihe, E., D. Nohr, S. Michel, S. Müller, H. J. Zentel, T. Fink, and J. Krekel. 1991. Molecular anatomy of the neuro-immune connection. *Int. J. Neurosci.* 59: 1–23.
52. Bergquist, J., A. Tarkowski, R. Ekman, and A. Ewing. 1994. Discovery of endogenous catecholamines in lymphocytes and evidence for catecholamine regulation of lymphocyte function via an autocrine loop. *Proc. Natl. Acad. Sci. USA* 91: 12912–12916.
53. Cosentino, M., A. M. Fietta, M. Ferrari, E. Rasini, R. Bombelli, E. Carcano, F. Saporiti, F. Meloni, F. Marino, and S. Lecchini. 2007. Human CD4+CD25+ regulatory T cells selectively express tyrosine hydroxylase and contain endogenous catecholamines subserving an autocrine/paracrine inhibitory functional loop. *Blood* 109: 632–642.
54. Capellino, S., M. Cosentino, C. Wolff, M. Schmidt, J. Grifka, and R. H. Straub. 2010. Catecholamine-producing cells in the synovial tissue during arthritis: modulation of sympathetic neurotransmitters as new therapeutic target. *Ann. Rheum. Dis.* 69: 1853–1860.
55. van Lent, P. L., C. G. Figdor, P. Barrera, K. van Ginkel, A. Slöetjes, W. B. van den Berg, and R. Torensma. 2003. Expression of the dendritic cell-associated C-type lectin DC-SIGN by inflammatory matrix metalloproteinase-producing macrophages in rheumatoid arthritis synovium and interaction with intercellular adhesion molecule 3-positive T cells. *Arthritis Rheum.* 48: 360–369.
56. Basu, S., and P. S. Dasgupta. 2000. Dopamine, a neurotransmitter, influences the immune system. *J. Neuroimmunol.* 102: 113–124.
57. Saha, B., A. C. Mondal, J. Majumder, S. Basu, and P. S. Dasgupta. 2001. Physiological concentrations of dopamine inhibit the proliferation and cytotoxicity of human CD4+ and CD8+ T cells in vitro: a receptor-mediated mechanism. *Neuroimmunomodulation* 9: 23–33.
58. Kipnis, J., M. Cardon, H. Avidan, G. M. Lewitus, S. Mordechay, A. Rolls, Y. Shani, and M. Schwartz. 2004. Dopamine, through the extracellular signal-regulated kinase pathway, downregulates CD4+CD25+ regulatory T-cell activity: implications for neurodegeneration. *J. Neurosci.* 24: 6133–6143.
59. Ramstad, C., V. Sundvold, H. K. Johansen, and T. Lea. 2000. cAMP-dependent protein kinase (PKA) inhibits T cell activation by phosphorylating ser-43 of raf-1 in the MAPK/ERK pathway. *Cell. Signal.* 12: 557–563.
60. Harada, Y., S. Miyatake, K.-i. Arai, and S. Watanabe. 1999. Cyclic AMP inhibits the activity of JNK (JNKp46) but not JNKp55 and ERK2 in human helper T lymphocytes. *Biochem. Biophys. Res. Commun.* 266: 129–134.
61. Vang, T., K. M. Torgersen, V. Sundvold, M. Saxena, F. O. Levy, B. S. Skålhegg, V. Hansson, T. Mustelin, and K. Taskén. 2001. Activation of the COOH-terminal Src kinase (Csk) by cAMP-dependent protein kinase inhibits signaling through the T cell receptor. *J. Exp. Med.* 193: 497–507.
62. Hershfield, M. S. 2005. New insights into adenosine-receptor-mediated immunosuppression and the role of adenosine in causing the immunodeficiency associated with adenosine deaminase deficiency. *Eur. J. Immunol.* 35: 25–30.
63. Jimenez, J. L., C. Punzón, J. Navarro, M. A. Muñoz-Fernández, and M. Fresno. 2001. Phosphodiesterase 4 inhibitors prevent cytokine secretion by T lymphocytes by inhibiting nuclear factor-kappaB and nuclear factor of activated T cells activation. *J. Pharmacol. Exp. Ther.* 299: 753–759.
64. Aandahl, E. M., W. J. Moretto, P. A. Haslett, T. Vang, T. Bryn, K. Tasken, and D. F. Nixon. 2002. Inhibition of antigen-specific T cell proliferation and cytokine production by protein kinase A type I. *J. Immunol.* 169: 802–808.
65. Korn, T., E. Bettelli, M. Oukka, and V. K. Kuchroo. 2009. IL-17 and Th17 Cells. *Annu. Rev. Immunol.* 27: 485–517.
66. Hashimoto, K., T. Inoue, T. Higashi, S.-i. Takei, T. Awata, S. Katayama, R. Takagi, H. Okada, and S. Matsushita. 2009. Dopamine D1-like receptor antagonist, SCH23390, exhibits a preventive effect on diabetes mellitus that occurs naturally in NOD mice. *Biochem. Biophys. Res. Commun.* 383: 460–463.
67. Okada, H., T. Inoue, K. Hashimoto, H. Suzuki, and S. Matsushita. 2009. D1-like receptor antagonist inhibits IL-17 expression and attenuates crescent formation in nephrotoxic serum nephritis. *Am. J. Nephrol.* 30: 274–279.

Continuation of Methotrexate Resulted in Better Clinical and Radiographic Outcomes Than Discontinuation upon Starting Etanercept in Patients with Rheumatoid Arthritis: 52-week Results from the JESMR Study

HIDETO KAMEDA, KATSUAKI KANBE, ERI SATO, YUKITAKA UEKI, KAZUYOSHI SAITO, SHOUHEI NAGAOKA, TOSHIHIKO HIDAKA, TATSUYA ATSUMI, MICHISHI TSUKANO, TSUYOSHI KASAMA, SHUNICHI SHIOZAWA, YOSHIYA TANAKA, HISASHI YAMANAKA, and TSUTOMU TAKEUCHI

ABSTRACT. ***Objective.*** The aim of the Efficacy and Safety of Etanercept on Active Rheumatoid Arthritis Despite Methotrexate Therapy in Japan (JESMR) study is to compare the efficacy of continuation versus discontinuation of methotrexate (MTX) when starting etanercept (ETN) in patients with active rheumatoid arthritis (RA).

Methods. In total, 151 patients with active RA who had been taking MTX were randomized to either ETN 25 mg twice a week with 6–8 mg/week MTX (the E+M group), or ETN alone (the E group). The primary endpoint at Week 52 was the radiographic progression assessed by van der Heijde-modified Sharp score.

Results. The mean progression in total score at Week 52 was not significantly different, statistically, between the E+M group and the E group (0.8 vs 3.6, respectively; $p = 0.06$). However, a significant difference was observed in radiographic progression between Weeks 24 and 52 (0.3 vs 2.5; $p = 0.03$), and the mean progression of the erosion score was negative in the E+M group, which was significantly better than the E group at Week 52 (–0.2 vs 1.8; $p = 0.02$). Clinically, the cumulative probability plot of the American College of Rheumatology (ACR)-N values at Week 52 clearly demonstrated a superior response in the E+M group than in the E group. ACR20, 50, and 70 response rates at Week 52 in the E+M group (86.3%, 76.7%, and 50.7%) were significantly greater than those in the E group (63.8%; $p = 0.003$, 43.5%; $p < 0.0001$ and 29.0%; $p = 0.01$, respectively).

Conclusion. MTX should be continued when starting ETN in patients with active RA. (ClinicalTrials.gov: NCT00688103) (First Release May 15 2011; J Rheumatol 2011;38:1585–92; doi:10.3899/jrheum.110014)

Key Indexing Terms:
METHOTREXATE RHEUMATOID ARTHRITIS TNFR-Fc FUSION PROTEIN

From the Japan Biological Agent Integrated Consortium (JBASIC); Division of Rheumatology, Keio University; Department of Orthopedics, Medical Center East, and Institute of Rheumatology, Tokyo Women's Medical University; Division of Rheumatology and Clinical Immunology, Showa University School of Medicine, Tokyo; Rheumatic and Collagen Disease Center, Sasebo Chuo Hospital, Sasebo; First Department of Internal Medicine, University of Occupational and Environmental Health, Kitakyushu; Department of Rheumatology, Yokohama Minami Kyosai Hospital, Yokohama; Institute of Rheumatology, Zenjinkai Shimin-No-Mori Hospital, Miyazaki; Department of Medicine II, Hokkaido University Graduate School of Medicine, Sapporo; Kumamoto Orthopaedic Hospital, Kumamoto; and The Center for Rheumatic Diseases, Kobe University Hospital, Kobe, Japan.

Supported by the Advanced Clinical Research Organization (Japan) and by research grants from the Japanese Ministry of Health, Labor and Welfare.

H. Kameda, MD, PhD, Assistant Professor; T. Takeuchi, MD, PhD, Professor, Division of Rheumatology, Keio University; K. Kanbe, MD, PhD, Associate Professor, Department of Orthopedics, Medical Center East, Tokyo Women's Medical University; E. Sato, MD; H. Yamanaka, MD, PhD, Professor, Institute of Rheumatology, Tokyo Women's Medical University; Y. Ueki, MD, PhD, Rheumatic and Collagen Disease Center, Sasebo Chuo Hospital; K. Saito, MD, PhD, Associate Professor; Y. Tanaka, MD, PhD, Professor, First Department of Internal Medicine, University of Occupational and Environmental Health; S. Nagaoka, MD, PhD, Department of Rheumatology, Yokohama Minami Kyosai Hospital; T. Hidaka, MD, PhD, Institute of Rheumatology, Zenjinkai Shimin-No-Mori Hospital; T. Atsumi, MD, PhD, Associate Professor, Department of Medicine II, Hokkaido University Graduate School of Medicine; M. Tsukano, MD, PhD, Kumamoto Orthopaedic Hospital; T. Kasama, MD, PhD, Associate Professor, Division of Rheumatology and Clinical Immunology, Showa University School of Medicine; S. Shiozawa, MD, PhD, Professor, The Center for Rheumatic Diseases, Kobe University Hospital.

Address correspondence to Dr. H. Kameda, Division of Rheumatology, Department of Internal Medicine, School of Medicine, Keio University, 35 Shinanomachi, Shinjuku-ku, Tokyo 160-8582, Japan.
E-mail: kamehide@z6.keio.jp

Full Release Article. For details see Reprints/Permissions at jrheum.org

Accepted for publication March 15, 2011.

The introduction of biological agents such as tumor necrosis factor-α (TNF-α) inhibitors into the therapeutic strategy for rheumatoid arthritis (RA) resulted in a shift characterized by the sufficient inhibition of arthritic signs and symptoms, radiographic progression, and functional disability[1,2]. However, the optimal use of those agents remains to be determined. For example, etanercept (ETN) has been shown to be effective for RA both as a monotherapy and as combination therapy with methotrexate (MTX), and the latter has proved its superiority to the former in MTX-naive patients. Because MTX is the first-line drug for most patients with RA, and ETN is much more expensive than MTX, ETN tends to be started for MTX-refractory, but not MTX-naive, patients in actual clinical practice[3,4].

The Add Enbrel or Replace Methotrexate (ADORE) trial was the first to consider whether adding ETN to MTX is better than replacing MTX with ETN. The trial failed to demonstrate the superiority of continuing MTX rather than discontinuing it upon starting ETN therapy[5]. Because the ADORE trial was only 16 weeks, with a regimen of MTX tapering over the initial 4 weeks, there could be no marked difference between continuation versus discontinuation of MTX, if any difference at all. Longterm efficacy and safety was not compared between the 2 groups.

Therefore, we conducted the Efficacy and Safety of Etanercept on Active Rheumatoid Arthritis Despite Methotrexate Therapy in Japan (JESMR) study to address the differences in clinical activity, radiographic progression, and functional disability over 2 years. The 24-week results from the JESMR study demonstrated that continuation of MTX after the start of ETN was better than discontinuation of MTX, in terms of European League Against Rheumatism (EULAR) response and American College of Rheumatology (ACR20) response rates[6]. We report the 52-week results, focusing on the radiographic progression measured by van der Heijde-modified Sharp (vdH-Sharp) score (which had been included in the co-primary endpoint), the ACR response[7], and functional disability evaluated by the Health Assessment Questionnaire-Disability Index (HAQ-DI)[8].

MATERIALS AND METHODS

Patients. Our prospective, randomized, open-label study was conducted at 45 institutions in Japan between June 2005 and January 2007. The study protocol (ClinicalTrials.gov: NCT00688103) was approved by an institutional ethics committee of each participating institute. All patients provided written informed consent in accord with the Declaration of Helsinki.

Patients had to be at least 18 years of age, had to fulfill the ACR 1987 revised classification criteria for RA, and had to meet the guidelines for the proper use of ETN in Japan [having at least 6 tender joints and 6 swollen joints, and either a serum C-reactive protein level of > 2 mg/dl or erythrocyte sedimentation rate (ESR) ≥ 28 mm at 1 h, with adequate safety profiles][9]. Precise inclusion and exclusion criteria have been reported[6].

Baseline characteristics of the patients were comparable between the ETN group (E group) and the ETN + MTX group (E+M group)[6]. More than 80% of the patients were women, at an average age of around 57 years, and with a disease duration of around 9 years (Table 1).

The rheumatoid factor was positive in about 90% of patients. The mean MTX dose at enrollment was 7 mg/week, with supplementary folic acid in 38%–52% of patients[6]. The baseline total vdH-Sharp score and its estimated yearly progression at study entry were very high in both groups, indicating the severity of disease of our patients (Table 1).

Procedures. Patients who had agreed to receive ETN for active RA were randomly assigned to continue MTX (6–8 mg/wk, an approved dose in Japan during the study period), that is, MTX + ETN combination therapy, or to discontinue MTX and switch to ETN monotherapy. Enrollment and randomization were performed on the University Hospital Medical Information Network Website (Tokyo, Japan) on the day of obtaining informed consent. Between June 2005 and January 2007, a total of 151 patients from 34 institutes in Japan were enrolled in the JESMR study. All patients enrolled were treated with ETN 25 mg as a subcutaneous injection twice weekly.

The co-primary endpoints of the JESMR study showed a good response according to the EULAR criteria, as based on a 28-joint Disease Activity Score (DAS28) and the ACR50 response rate at Week 24, as reported[6], and the radiographic progression assessed by vdH-Sharp score ranged from 0 to 448 over 52 weeks[10]. Two trained readers independently scored each radiograph of hands and feet at baseline and at Weeks 24 and 52. Patient identities and treatment groups were blinded to the readers, although the chronological sequence of the radiographs in sets was unmasked. The smallest detectable difference between readers at baseline was 9.9 (standard deviation of the per-patient difference between the readers divided by the square root of 2), and the smallest detectable change over 52 weeks was 1.9.

Statistical analysis. A sample size of 150 patients per treatment group was first calculated to provide > 90% power ($\alpha = 0.05$, $\beta = 0.1$) with 15% non-completion rate during 24 weeks. This calculation assumed that the ACR50 response rate would be 40% in the E group and 60% in the E+M group. However, because of the delay in patient recruitment, we completed the patient enrollment in January 2005 at a total of 151 patients (74 in the E group and 77 in the E+M group). This decision was based on the calculation that a sample size of 64 per treatment group was needed to provide more than 90% power ($\alpha = 0.05$, $\beta = 0.1$), assuming that the mean radiographic progression by vdH-Sharp score at 52 weeks would be 1.50 in the E group and –0.80 in the E+M group.

Efficacy analyses included all patients who took the study drugs and had a valid baseline and ≥ 1 on-therapy value for each endpoint. The last observation carried forward (LOCF) and linear imputation were used for the analysis of clinical and radiographic efficacy, respectively, for missing data. All analyses were performed by the CMIC Co. Ltd. Data Center (Osaka, Japan). The proportions of participants who met given criteria were compared with Fisher's exact test, while the mean values between the groups were compared with the Mann-Whitney U test.

RESULTS

Primary endpoint: radiographic efficacy. Efficacy analysis was performed in 69 patients of the E group and 73 of the E+M group (Figure 1). The rate of per-protocol patients was smaller in the E group than in the E+M group, chiefly because of a lack of efficacy after 24 weeks.

The baseline vdH-Sharp score was 114.5 ± 85.7 in the E group and 113.1 ± 85.6 in the E+M group ($p = 0.99$). Cumulative probability plot analysis suggested less overall radiographic progression in the E+M group than in the E group during the 52 weeks (Figure 2A). However, the primary endpoint at 52 weeks was not met because the numerical superiority of the E+M group over the E group in the change in vdH-Sharp score over 52 weeks did not reach a statistically significant difference (0.8 vs 3.6, respectively; $p = 0.06$), as shown in Figure 2B. Nonetheless, the mean progression in the erosion score was negative exclusively in the E+M group, at

Table 1. Demographic features of the patients. Except where indicated otherwise, values are mean ± SD.

Characteristics	ETN, n = 71	ETN + MTX, n = 76	p
Age, yrs	58.1 ± 12.6	56.6 ± 11.1	0.23
Women, %	87.3	80.3	0.27
Body weight, kg	51.0 ± 8.4	54.6 ± 11.3	0.057
Disease duration, yrs	10.6 ± 10.5	8.0 ± 7.6	0.21
Positive rheumatoid factor, %	91.5	86.7	0.43
MTX dose, mg/wk	7.0 ± 1.4	7.4 ± 1.1	0.099
Total vdH-Sharp score, (median; IQR)	114.5 ± 85.7 (94.5; 120.0)	113.1 ± 85.6 (89.5; 91.0)	0.99
Estimated yearly progression, (median; IQR)	17.7 ± 13.2 (13.9; 16.0)	20.8 ± 18.2 (4.4; 12.2)	0.45
Erosion score, (median; IQR)	55.6 ± 53.0 (43.5; 59.5)	56.6 ± 54.4 (37.8; 53.0)	0.80
Joint space narrowing score, (median; IQR)	58.9 ± 33.9 (54.0; 55.0)	56.5 ± 32.9 (47.8; 41.4)	0.79

ETN: etanercept; MTX: methotrexate; vdH: van der Heijde; IQR: interquartile range.

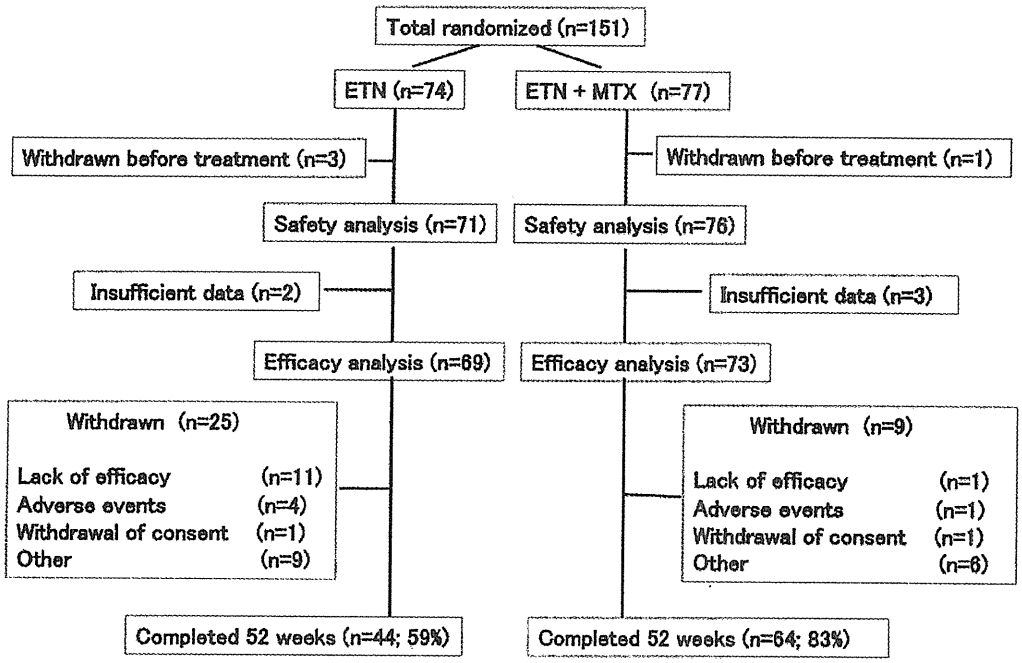

Figure 1. Disposition of patients during 52 weeks of the Efficacy and Safety of Etanercept on Active Rheumatoid Arthritis Despite Methotrexate Therapy in Japan (JESMR) study. A total of 151 patients were enrolled, 74 in the etanercept (ETN) group and 77 in the etanercept and methotrexate (MTX) group, and 108 patients (71.5%) completed 52 weeks per protocol.

both 24 weeks and 52 weeks (–0.1 and –0.2, respectively), and it was significantly better than that in the E group at 52 weeks (1.8; p = 0.02). Moreover, a significant difference was observed in the total score progression between Weeks 24 and 52 (2.5 in the E group and 0.3 in the E+M group; p = 0.03), suggesting the carrying-over effect of MTX for the initial few months.

The proportion of patients showing no radiographic progression over 52 weeks (change in vdH-Sharp score ≤ 0.5) was 39.6% in the E group and 57.4% in the E+M group (p = 0.07), and the proportion showing no clinically significant radiographic progression (change in vdH-Sharp score ≤ smallest detectable change) was 58.5% in the E group and 67.6% in the E+M group (p = 0.34).

Clinical efficacy. Next we performed for the first time a cumulative probability plot analysis of ACR-N values at 52 weeks for both treatment groups (Figure 3). This analysis clearly demonstrated the superior clinical response in the E+M group compared to the E group, and implied that the continuation of MTX would be beneficial, at least to some extent, in nearly 80% of patients upon the commencement of ETN. Indeed, the mean ± SD of ACR-N was 60.9 ± 29.3 for the E+M group, which was significantly greater than that of the E group (31.1 ± 50.8; p = 0.0003). In addition, the area under the curve of the ACR-N throughout 52 weeks was also significantly different between the groups (26.8 ± 13.0 in the E+M group and 18.4 ± 19.0 in the E group; p = 0.008). At the same time, we could easily see the superior ACR response rates in the E+M

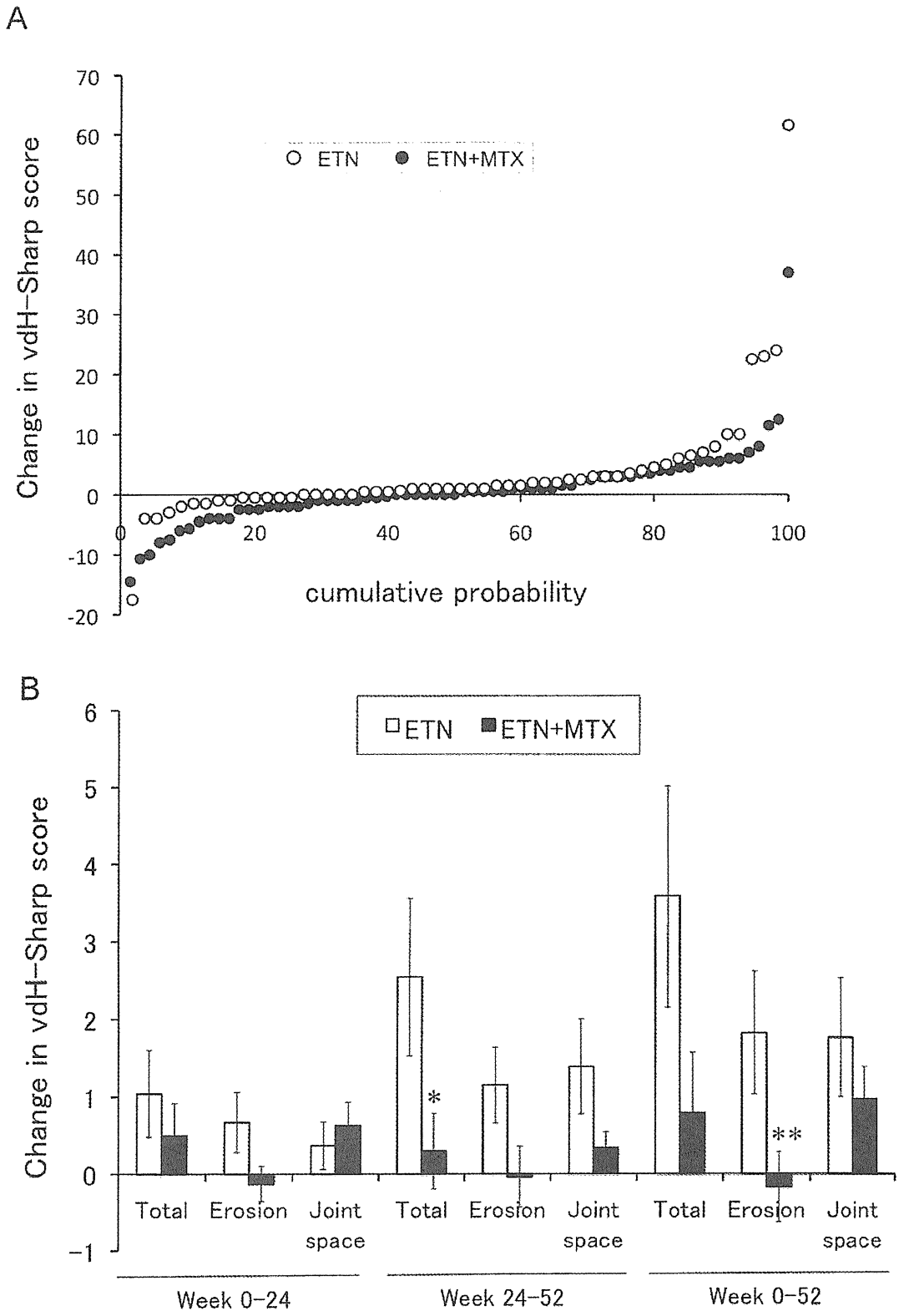

Figure 2. Change in van der Heijde-modified Sharp (vdH-Sharp) total score represented by cumulative probability plot (A) and the mean change of total score as well as erosion and joint space narrowing scores (B) over 52 weeks. Values are mean ± SEM, compared by Mann-Whitney U test (*p = 0.03; **p = 0.02) between groups. ETN: etanercept group; ETN+MTX: etanercept plus methotrexate group.

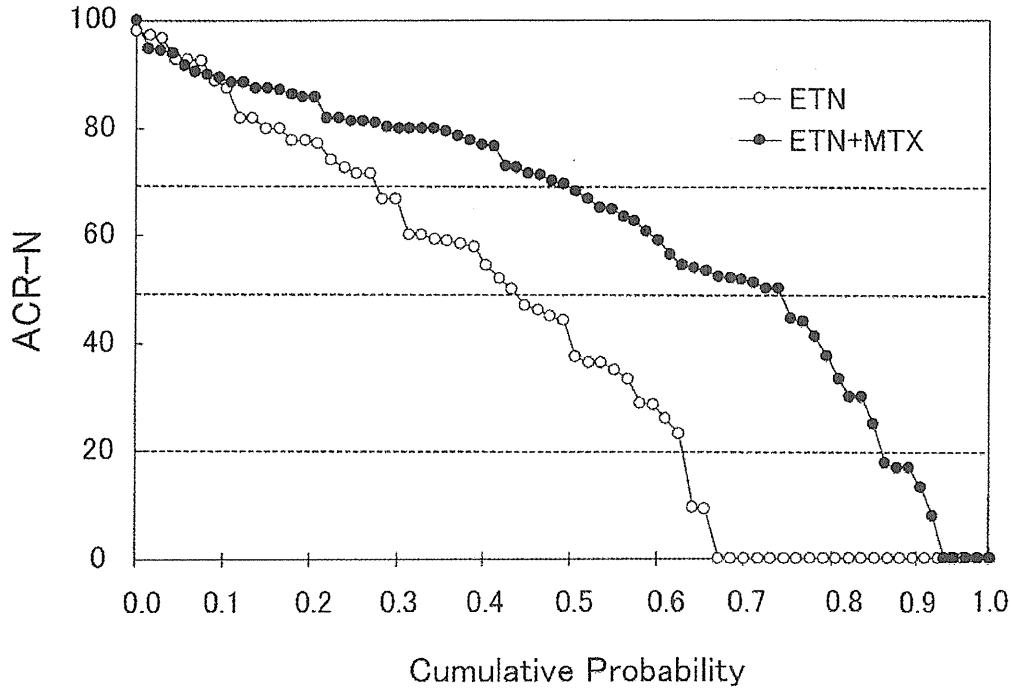

Figure 3. American College of Rheumatology (ACR) values at 52 weeks; 69 patients in the etanercept group (ETN) and 73 in the etanercept plus methotrexate group (ETN+MTX) were analyzed. Broken lines indicate ACR20, ACR50, and ACR70 values.

group compared to the E group, as shown in Figure 3: 86.3% vs 63.8% in ACR20 ($p = 0.003$), 76.7% vs 43.5% in ACR50 ($p < 0.0001$), and 50.7% vs 29.0% in ACR70 ($p = 0.01$), respectively (Table 2). Except for patient global assessment, all important clinical measures, including HAQ-DI, favored the continuation of MTX at Week 52, as shown in Table 2.

Safety analyses. Safety profiles between the 2 treatment groups were comparable (Table 3). Similar overall adverse events were observed between the treatment groups. The frequency of general disorders and administration site conditions, mostly injection site reaction (13 in the E group and 7 in the E+M group), tended to be higher in the E group than the E+M group, as well as skin and subcutaneous tissue disorders including eczema and erythema developed at sites unrelated

Table 2. Comparison of the clinical responses between treatment groups. Except where indicated otherwise, values are mean ± SD.

Measures	ETN, n = 69			MTX + ETN, n = 73			p at 52 Weeks
	0 Week	52 Weeks	p	0 Week	52 Weeks	p	Between Groups
Tender joint count (68 assessed)	15.0 ± 9.4	4.3 ± 5.3	< 0.0001	15.1 ± 8.1	2.1 ± 2.8	< 0.0001	0.020
Swollen joint count (66 assessed)	12.4 ± 6.1	4.0 ± 4.4	< 0.0001	12.5 ± 6.5	1.8 ± 2.3	< 0.0001	0.008
Patient global assessment	62.5 ± 20.5	27.4 ± 25.1	< 0.0001	53.7 ± 23.7*	21.3 ± 19.4	< 0.0001	0.264
ESR, mm/l h	59.7 ± 28.4	43.7 ± 27.0	< 0.0001	59.5 ± 26.5	28.9 ± 23.8	0.0002	0.0002
CRP, mg/dl	2.5 ± 2.5	1.3 ± 1.6	< 0.0001	3.0 ± 3.2	0.5 ± 0.8	< 0.0001	0.0003
DAS28	6.1 ± 0.9	4.2 ± 1.5	< 0.0001	6.0 ± 1.0	3.0 ± 1.0	< 0.0001	< 0.0001
EULAR good response, %	—	33.3	—	—	52.1	—	< 0.0001
DAS28 < 2.6, %	0	18.8	—	0	35.6	—	0.038
ACR20 responder, %	—	63.8	—	—	86.3	—	0.0003
ACR50 responder, %	—	43.5	—	—	76.7	—	< 0.0001
ACR70 responder, %	—	29	—	—	50.7	—	0.001
HAQ-DI	1.3 ± 0.8	0.9 ± 0.7	< 0.0001	1.2 ± 0.7	0.6 ± 0.6	< 0.0001	0.041

* A significant difference between groups was observed at Week 0 (about 4 weeks after enrollment shown in Table 1) for patient's global assessment value, in which p value was 0.025. ETN: etanercept; MTX: methotrexate; ESR: erythrocyte sedimentation rate; CRP: C-reactive protein; DAS28: 28-joint Disease Activity Score; EULAR: European League Against Rheumatism; ACR: American College of Rheumatology; HAQ-DI: Health Assessment Questionnaire-Disability Index.

Table 3. Adverse events. Values are numbers of patients who developed (serious) adverse events.

Type of Adverse Event	ETN, n = 71	ETN + MTX, n = 76	p
Blood and lymphatic system disorders	2	0	0.232
Cardiac disorders	0	1 (1)	1.000
Eye disorders	1	2	1.000
Gastrointestinal disorders	7	5	0.554
General disorders and administration site conditions	15	7	0.063
Hepatobiliary disorders	1	5	0.211
Infections and infestations	19	21 (2)	1.000
Injury, poisoning, procedural complications	3 (2)	5 (3)	0.720
Metabolism and nutrition disorders	1	2	1.000
Musculoskeletal and connective tissue disorders	2	0	0.232
Neoplasms benign, malignant, unspecified	0	1 (1)	1.000
Nervous system disorders	2	4 (1)	0.682
Psychiatric disorders	3	3	1.000
Renal and urinary disorders	0	1	1.000
Reproductive system and breast disorders	0	1	1.000
Respiratory, thoracic, mediastinal disorders	3	2	0.673
Skin and subcutaneous tissue disorders	11	5	0.112
Vascular disorders	1	0	0.483
Serious adverse events	2	7	0.168

ETN: etanercept; MTX: methotrexate.

to ETN injection. In contrast, the frequency of hepatobiliary disorders, mostly liver dysfunction, tended to be higher in the E+M group than in the E group. The result was the same between the groups with metabolism and nutrition disorders such as hyperlipidemia, diabetes mellitus, and hyperuricemia. Serious adverse events in the E group were bone fractures in 2 patients (humeral bone and osteoporotic vertebrae). Serious adverse events in the E+M group were bone fractures in 3 (femoral bone in 2, cranial bone in 1), and in 1 patient each, congestive heart failure, cellulitis, herpes zoster, brain hemorrhage, and mammary carcinoma. Cranial bone fracture from a traffic accident and cellulitis developed in the same patient. Treatment was withdrawn because of injection site reaction in 4 patients in the E group and mammary carcinoma in 1 patient in the E+M group. Thus, the safety profile was comparable between 2 groups.

DISCUSSION

In a previous report on the 24-week results of the JESMR study, the superiority of a continuation of MTX over its discontinuation when starting ETN in terms of controlling clinical disease activity (the rates of EULAR good response, remission, and ACR20 response, but not ACR50 and 70 responses) was indicated[6]. Our 52-week results not only confirmed the previous ones but also proved, for the first time, that the combination of ETN and MTX resulted in a better outcome in radiographic progression determined by vdH-Sharp score, especially in erosions, even in patients who had shown an incomplete response to MTX. The mean progression in total score at Week 52 was not significantly different, statistically, between the E+M group and the E group (0.8 vs 3.6, respectively; p = 0.06). The chief reason for failure to achieve the primary endpoint seemed to be the reduction in sample size due to delayed recruitment of patients. However, a significant difference was observed in radiographic progression between Weeks 24 and 52 (0.3 vs 2.5, respectively; p = 0.03), and the mean progression of the erosion score was negative in the E+M group, which was significantly better than the E group at Week 52 (–0.2 vs 1.8, respectively; p = 0.02). Further, all important clinical measures, including ACR responses, EULAR responses, and HAQ-DI, favored the continuation of MTX at Week 52.

Infliximab was the first biological agent to have demonstrated complete inhibition of radiographic progression in combination with MTX in MTX-refractory patients with active RA[11]. ETN and adalimumab showed similar efficacy in halting joint destruction in combination with MTX. Both agents proved their superior clinical and radiographic efficacy with MTX combination over monotherapy in MTX-naive patients with early RA (the PREMIER study[12]) or established RA (the TEMPO study[13]). Our results led to the conclusion that anti-TNF biological agents should be used in combination with MTX as far as possible, whether the patients are MTX-naive or MTX-refractory, and they strongly support the recent recommendations of the ACR[3] and EULAR[4].

The reason that the continuation of MTX, which had only shown an inadequate response in the enrolled patients, demonstrated a significant effect with ETN treatment may be as follows: (1) the efficacy of MTX was insufficient but not negligible even as a monotherapy; and (2) the targets of MTX, including activated T cells[14], are not identical to those of ETN, resulting in additive or synergistic effects between MTX and ETN. A recent report from the GO-FORWARD study also

demonstrated a better clinical response to golimumab with MTX continuation than with its discontinuation in MTX-refractory patients with RA[15]. The fact that many clinical (ACR50 and 70 response rates and HAQ-DI score) and radiographic (erosion score progression) measures showed statistically significant differences at Week 52 but not at Week 24[6] may explain why the ADORE study did not show a difference between MTX continuation and discontinuation[5,16]. The usefulness of MTX continuation seems to be true with all biological agents targeting TNF.

The average disease duration of about 9 years significantly affected the radiographic and HAQ-DI results in the JESMR study. Despite a long disease duration, our patients showed a rapid progression in vdH-Sharp scores with a mean estimated yearly progression of 18–21 (Table 1). This result was close to that of patients with early active RA who were enrolled in the PREMIER study (26–27)[12] and was much higher than that in the TEMPO study (8–11)[13]. This fact may explain, at least in part, the similarities and differences in the radiographic progression results among those clinical trials. In addition, the radiographic progression in our patients could be more aggressive in the initial few years after disease onset. Therefore, whether our results are also true for patients with early RA of < 6 months' duration should be examined in the near future.

Most of the adverse events, including infections and skin disorders other than injection site reactions, were observed throughout 52 weeks. However, as expected, injection site reaction was less frequent after 24 weeks when compared to our previous report[6]. In contrast, most of the bone fractures, which were the predominant serious adverse events in our study, developed after 24 weeks. This could be attributed at least in part to the improved activity of daily life of our patients treated with ETN as demonstrated by the HAQ-DI improvement (Table 2).

Our study has several limitations. First, it was not double-blinded. Therefore, one may assume there was an awareness of the treatment effect evaluations by physicians and by patients. However, the changes in acute-phase reactants (Table 2) and radiographic results (Figures 2A and 2B) make that unlikely. Further, there were considerable withdrawal rates in the E group (Figure 1), mostly because of a lack of efficacy after 24 weeks. Since this had been expected, because this study was not double-blinded, we applied the LOCF methods for clinical efficacy analyses instead of intention-to-treat analyses. In addition, the sample size of the JESMR study limited the power of detection of differences between the 2 treatment groups. Actual ACR50 response rates and the radiographic progression were greater than our expectations in both treatment groups. Finally, the dose of MTX approved by the Japanese Ministry of Health, Labor and Welfare had been only 6–8 mg/week throughout this study[17,18] although, concordantly, the use of supplementary folic acid was also limited to about half of the patients receiving MTX. In February 2011, the Ministry approved MTX use up to 16 mg/week for patients with RA. Nonetheless, overall clinical and radiographic outcomes of infliximab added to MTX 7–9 mg/week in Japan[19,20,21,22,23] were comparable to those in the ATTRACT[11] and ASPIRE studies[24].

Future studies may also include the prediction of patient outcome after the start of ETN therapy, addressing the question of who can be sufficiently controlled by simply switching from MTX to ETN, and who can be sufficiently controlled by the addition of ETN to MTX but not by switching from MTX to ETN. These subanalyses are now under investigation in the Japan Biological Agent Integrated Consortium (JBASIC) study group.

Our results demonstrated for the first time that the continuation of MTX resulted in a better clinical and radiographic outcome, at least in some aspects, than its discontinuation after the start of ETN in patients with active RA despite MTX therapy. We also showed the usefulness of cumulative probability plot presentation not only for radiographic progression but also for clinical responses such as ACR-N, which may be included in future clinical trials.

ACKNOWLEDGMENT

We acknowledge the following investigators, their staff and all institutions, affiliated and otherwise: K. Shiozawa (Konan Kakogawa Hospital); S. Kobayashi (Juntendo University School of Medicine, Koshigaya Hospital); N. Tamura (Juntendo University School of Medicine, Juntendo Hospital); T. Sawada (The University of Tokyo Hospital); S. Yamana (Higashihiroshima Memorial Hospital); Y. Honda (Kurume University Hospital); T. Kojima (Nagoya University Hospital); H. Takahashi (Sapporo Medical University Hospital); T. Sugiyama (Shimoshizu National Hospital); A. Taniguchi (Tokyo Women's Medical University, Institute of Rheumatology); T. Nanki (Tokyo Medical and Dental University Hospital, Faculty of Medicine); M. Yamamura (Aichi Medical University Hospital); K. Kurasawa (Dokkyo Medical University Hospital); K. Chiba (Fukushima Daiichi Hospital); K. Kato (Fujita Health University Hospital); K. Ezawa (Kurashiki Kousai Hospital); T. Fujii (Kyoto University Hospital); S. Nakata (Matsuyama Red Cross Hospital); S. Tamachi (Mie Chuo Medical Center); Y. Kawabe (National Hospital Organization Ureshino Medical Center); R. Yano (Okayama University Hospital); T. Kuroiwa (The Hospital of Hyogo College of Medicine); A. Kubota (Toho University Omori Medical Center); Hyogo Prefectural General Rehabilitation Center; Rokko Island Hospital; Kurume University Medical Center; Nagasaki University Hospital of Medicine and Dentistry; Nihon University Itabashi Hospital; Niigata University Medical and Dental Hospital; Osaki Citizens' Hospital; Saiseikai Takaoka Hospital; St. Marianna University School of Medicine Hospital; Taihakusakura Hospital; Tohoku Kosei Nenkin Hospital; Tohoku University Hospital; and Tsukuba University Hospital.

REFERENCES

1. Keystone EC. Strategies to control disease in rheumatoid arthritis with tumor necrosis factor antagonists — an opportunity to improve outcomes. Nat Clin Pract Rheumatol 2006;2:594-601.
2. Smolen JS, Aletaha D, Koeller M, Weisman MH, Emery P. New therapies for treatment of rheumatoid arthritis. Lancet 2007;370:1861-74.
3. Saag KG, Teng GG, Patkar NM, Anuntiyo J, Finney C, Curtis JR, et al. American College of Rheumatology 2008 recommendations for the use of nonbiologic and biologic disease-modifying antirheumatic drugs in rheumatoid arthritis. Arthritis Rheum

2008;59:762-84.
4. Smolen JS, Landewé R, Breedveld FC, Dougados M, Emery P, Gaujoux-Viala C, et al. EULAR recommendations for the management of rheumatoid arthritis with synthetic and biological disease-modifying antirheumatic drugs. Ann Rheum Dis 2010;69:964-75.
5. van Riel PL, Taggart AJ, Sany J, Gaubitz M, Nab HW, Pedersen R, et al. Efficacy and safety of combination etanercept and methotrexate versus etanercept alone in patients with rheumatoid arthritis with an inadequate response to methotrexate: the ADORE study. Ann Rheum Dis 2006;65:1478-83.
6. Kameda H, Ueki Y, Saito K, Nagaoka S, Hidaka T, Atsumi T, et al. Etanercept (ETN) with methotrexate (MTX) is better than ETN monotherapy in patients with active rheumatoid arthritis despite MTX therapy: a randomized trial. Mod Rheumatol 2010;20:531-8.
7. Bathon JM, Martin RW, Fleischmann RM, Tesser JR, Schiff MH, Keystone EC, et al. A comparison of etanercept and methotrexate in patients with early rheumatoid arthritis. N Engl J Med 2000;343:1586-93.
8. Fries JF, Spitz P, Kraines RG, Holman HR. Measurement of patient outcome in arthritis. Arthritis Rheum 1983;26:1346-53.
9. Miyasaka N, Takeuchi T, Eguchi K. Guidelines for the proper use of etanercept in Japan. Mod Rheumatol 2006;16:63-7.
10. van der Heijde D. How to read radiographs according to the Sharp/van der Heijde method. J Rheumatol 2000;27:261-3.
11. Lipsky PE, van der Heijde DM, St. Clair EW, Furst DE, Breedveld FC, Kalden JR, et al. Infliximab and methotrexate in the treatment of rheumatoid arthritis. N Engl J Med 2000;343:1594-602.
12. Breedveld FC, Weisman MH, Kavanaugh AF, Cohen SB, Pavelka K, van Vollenhoven R, et al. The PREMIER study: A multicenter, randomized, double-blind clinical trial of combination therapy with adalimumab plus methotrexate versus methotrexate alone or adalimumab alone in patients with early, aggressive rheumatoid arthritis who had not had previous methotrexate treatment. Arthritis Rheum 2006;54:26-37.
13. Klareskog L, van der Heijde D, de Jager JP, Gough A, Kalden J, Malaise M, et al. Therapeutic effect of the combination of etanercept and methotrexate compared with each treatment alone in patients with rheumatoid arthritis: double-blind randomized controlled trial. Lancet 2004;363:675-81.
14. Braun J, Rau R. An update on methotrexate. Curr Opin Rheumatol 2009;21:216-23.
15. Keystone EC, Genovese MC, Klareskog L, Hsia EC, Hall ST, Miranda PC, et al. Golimumab, a human antibody to tumour necrosis factor a given by monthly subcutaneous injections, in active rheumatoid arthritis despite methotrexate therapy: the GO-FORWARD Study. Ann Rheum Dis 2009;68:789-96.
16. van Riel PL, Freundlich B, MacPeek D, Pedersen R, Foehl JR, Singh A, et al. Patient-reported health outcomes in a trial of etanercept monotherapy versus combination therapy with etanercept and methotrexate for rheumatoid arthritis: the ADORE trial. Ann Rheum Dis 2008;67:1104-10.
17. Kameda H, Amano K, Sekiguchi N, Takei H, Ogawa H, Nagasawa H, et al. Factors predicting the response to low-dose methotrexate therapy in patients with rheumatoid arthritis: a better response in male patients. Mod Rheumatol 2004;14:442-6.
18. Takeuchi T, Kameda H. The Japanese experience with biologics. Nat Rev Rheumatol 2010;6:644-52.
19. Kameda H, Sekiguchi N, Nagasawa H, Amano K, Takei H, Suzuki K, et al. Development and validation of handy rheumatoid activity score with 38 joints (HRAS38) in rheumatoid arthritis patients receiving infliximab. Mod Rheumatol 2006;16:381-8.
20. Yamanaka H, Tanaka Y, Sekiguchi N, Inoue E, Saito K, Kameda H, et al. Retrospective study on the notable efficacy and related factors of infliximab therapy in a rheumatoid arthritis management group in Japan (RECONFIRM). Mod Rheumatol 2007;17:28-32.
21. Tanaka Y, Takeuchi T, Inoue E, Saito K, Sekiguchi N, Sato E, et al. Retrospective study on the notable efficacy and related factors of infliximab therapy in a rheumatoid arthritis management group in Japan: one-year clinical outcome (RECONFIRM-2). Mod Rheumatol 2008;18:146-52.
22. Takeuchi T, Yamanaka H, Inoue E, Nagasawa H, Nawata M, Ikari K, et al. Retrospective clinical study on the notable efficacy and related factors of infliximab therapy in a rheumatoid arthritis management group in Japan: One-year outcome of joint destruction (RECONFIRM-2J). Mod Rheumatol 2008;18:447-52.
23. Tanaka Y, Takeuchi T, Mimori T, Saito K, Nawata M, Kameda H, et al. Discontinuation of infliximab after attaining low disease activity in patients with rheumatoid arthritis: RRR (remission induction by Remicade in RA) study. Ann Rheum Dis 2010;69:1286-91.
24. St. Clair EW, van der Heijde DM, Smolen JS, Maini RN, Bathon JM, Emery P, et al. Combination of infliximab and methotrexate therapy for early rheumatoid arthritis. A randomized, controlled trial. Arthritis Rheum 2004;50:3432-43.

Phenotypic Changes of Lymphocytes in Patients with Systemic Lupus Erythematosus Who Are in Longterm Remission After B Cell Depletion Therapy with Rituximab

SHIGERU IWATA, KAZUYOSHI SAITO, MIKIKO TOKUNAGA, KUNIHIRO YAMAOKA, MASAO NAWATA, SONOSUKE YUKAWA, KENTARO HANAMI, SHUNSUKE FUKUYO, IPPEI MIYAGAWA, SATOSHI KUBO, and YOSHIYA TANAKA

ABSTRACT. ***Objective.*** Rituximab has recently emerged as a novel treatment strategy for systemic lupus erythematosus (SLE). We investigated longitudinally the differentiation and phenotypic changes of peripheral B cells and T cells in patients with SLE after rituximab treatment.

Methods. Phenotypic changes on B cells and T cells in 10 patients with SLE treated with rituximab were analyzed before, 28 days after, and 2 years after rituximab treatment, and at relapse.

Results. Rituximab rapidly depleted naive and memory B cells from the peripheral blood. In the patients with prolonged remission, the memory B cells remained depleted while naive B cells recovered within 3–9 months, and the expression levels of CD40 and CD80 remained downregulated for 2 years. There was also a decrease of memory T cells relative to naive T cells, and the expression of CD40L and inducible costimulator (ICOS) on CD4-positive T cells rapidly decreased and remained downregulated for 2 years. In 1 patient, an increase in the number of memory B cells with upregulation of CD40 and CD80 expression was noted just before relapse. In another patient with relapse, however, recovery of CD4-positive memory T cells with upregulation of ICOS expression was noted, with no change in the number of memory B cells.

Conclusion. Our results suggest that the phenotypic changes of peripheral B cells result in inhibition of T cell differentiation and activation mediated by B cells and thereby bring about longterm remission of SLE. Activated memory B cells or ICOS-positive CD4-positive memory T cells reappeared in association with relapse, probably reflecting the heterogeneity of SLE. (First Release Dec 15 2010; J Rheumatol 2011;38:633–41; doi:10.3899/jrheum.100729)

Key Indexing Terms:
SYSTEMIC LUPUS ERYTHEMATOSUS RITUXIMAB B CELL DEPLETION THERAPY

Systemic lupus erythematosus (SLE) is a multisystem autoimmune disease induced by activation of autoreactive T cells and overproduction of autoantibodies by B cells. Rituximab is a human-mouse chimeric monoclonal antibody that targets the CD20 antigen, a B cell-specific antigen, and causes depletion of CD20-expressing pre-B to mature B cells. Rituximab has recently been reported to show a rapid onset of effect and prolonged efficacy in patients with refractory SLE[1,2,3,4,5,6,7,8], emerging as a promising new agent for the treatment of this disease. In regard to the mechanism underlying the longterm remission of SLE induced by rituximab, Anolik, *et al*[9] reported that the drug caused peripheral blood depletion of memory B cells[10,11] and plasma cells[12] that play important roles in the pathogenesis of SLE, as well as a depletion of memory B cells from the secondary lymphoid tissue[13].

It has been reported that not only activated B cells, but also T cells and dendrocytes are involved in the pathogenesis of SLE in humans[14,15,16,17]. Treatment with rituximab has been demonstrated to produce an increase in the number of CD4+CD25^{bright}Foxp3+ regulatory T cells in the peripheral blood during the recovery phase from SLE or an increase in the messenger RNA expression of Foxp3 at 1 to

From the First Department of Internal Medicine, School of Medicine, University of Occupational and Environmental Health, Kitakyushu, Japan.

Supported in part by a Research Grant-In-Aid for Scientific Research from the Ministry of Health, Labor and Welfare of Japan, the Ministry of Education, Culture, Sports, Science and Technology of Japan, and the University of Occupational and Environmental Health, Japan. Dr. Tanaka has received consultant fees from Mitsubishi-Tanabe Pharma and Pfizer Inc. and lecture fees from Mitsubishi-Tanabe Pharma, Takeda Pharmaceutical Co. Ltd., Abbott, Eisai Pharma, and Chugai Pharma.

S. Iwata, MD; K. Saito, MD, PhD; M. Tokunaga, MD, PhD; K. Yamaoka, MD, PhD; M. Nawata, MD; S. Yukawa, MD; K. Hanami, MD; S. Fukuyo, MD; I. Miyagawa, MD; S. Kubo, MD; Y. Tanaka, MD, PhD, First Department of Internal Medicine, School of Medicine, University of Occupational and Environmental Health.

Address correspondence to Prof. Y. Tanaka, The First Department of Internal Medicine, School of Medicine, University of Occupational and Environmental Health, 1-1 Iseigaoka, Yahata-nishi, Kitakyushu 807-8555, Japan. E-mail: tanaka@med.uoeh-u.ac.jp

Accepted for publication October 12, 2010.

3 months after treatment[18,19]. We have also shown that rituximab may downregulate the expression of CD40L, a costimulatory molecule expressed on T cells, in patients with SLE[7]. To our knowledge, however, there are no reported comprehensive studies that have investigated the effects of rituximab on the differentiation of T and B cells or on the expression of costimulatory molecules on these cells. The precise mechanisms underlying the longterm remission of SLE induced by rituximab and the lymphocyte subsets involved in the pathogenesis of SLE remain unknown.

We investigated longitudinally the pattern of B cell and T cell differentiation and the changes in the expression levels of costimulatory molecules on these cells in rituximab-treated patients with SLE showing longterm remission and relapse, in order to determine the mechanisms underlying both the longterm remission of SLE induced by rituximab and the lymphocyte subsets involved in the pathogenesis of SLE.

MATERIALS AND METHODS

Patients. Our cohort study involved 10 patients diagnosed with SLE based on their fulfilling at least 4 of the 11 modified American College of Rheumatology (ACR) criteria for the diagnosis of SLE[20]. Table 1 shows the background variables of the patients before they started rituximab treatment. The subjects were 9 women and 1 man, with a mean age of 27.4 ± 8.8 years (range 16–41 yrs). The mean duration of illness from SLE diagnosis to administration of rituximab was 96.7 ± 113.3 months (range 3–324 mo). The mean steroid dose prior to the start of rituximab treatment was 35.0 ± 16.8 mg/day. Despite receiving conventional treatments such as pulse steroid therapy, intermittent intravenous cyclophosphamide pulse therapy (IVCY), cyclosporine A, mizoribine, azathioprine, mycophenolate, plasma exchange, and immunoadsorption therapy, all the patients had highly active disease, with a mean SLE Disease Activity Index (SLEDAI) of 16.2 ± 9.6 and a British Isles Lupus Assessment Group (BILAG) activity index of 19.8 ± 8.2 (all patients falling in the BILAG score category) at the start of rituximab treatment. The organ involvement was as follows: lupus nephritis in 7 patients [World Health Organization (WHO) type I in 1 patient and type IV in 6 patients], neuropsychiatric SLE in 5 patients, and thrombotic thrombocytopenic purpura in 1 patient. All patients were treated with rituximab at our facility between 2004 and 2009, and all completed the course of the anti-CD20 antibody treatment protocol formulated for our study. Written informed consent was obtained from each patient in accord with the requirement of the study protocol approved by the ethics committee of our university.

Treatment schedule. Rituximab was administered twice, with a 1-week interval between administrations, at a dose of 375 mg/m^2 in all patients.

Assessment. Laboratory measurements included the serum levels of complements, and the titers of antinuclear antibody, antiribonucleoprotein antibody, anti-SSA antibody, anti-SSB antibody, anti-Sm antibody, and anti-dsDNA antibody. To assess the activity of SLE, the BILAG index[21] and SLEDAI[22] were calculated. Disease activity was scored on a 5-category scale by the BILAG index: A (severely active), B (moderately active), C (stable mild disease), D, and E. Responses to rituximab were categorized according to the improvement of the BILAG index, as major clinical response (MCR), partial clinical response (PCR), and no clinical response (NCR). More specifically, MCR was defined as improvement of the BILAG index to C or better at 2 years, PCR as improvement of the BILAG index to B in at least 1 domain at 2 years, and NCR as failure to meet the definition of either MCR or PCR[5].

Flow cytometry. Analysis of the B cell and T cell phenotypes and expression of the surface molecules on these cells was carried out by flow cytometry before, 28 days after, and 2 years after rituximab treatment, as well as at the time of relapse. Mononucleated cells were isolated from the peripheral blood, and were treated with the following antibodies:

Table 1. Characteristics of the study participants with systemic lupus erythematosus.

Patient	Age, yrs/ Sex	Disease Duration, mo	CS Dose, mg	Treatments Prior to RTX	Organ Involvement	Anti-dsDNA antibody, IU/ml	ENA	C3/C4/CH50	ANA	CS Dose at 2 yrs	SLEDAI Day 0 to 2 yrs	BILAG Day 0 to 2 yrs	Clinical Response at 2 yrs
1	39 F	144	22.5	IVCY, CsA	nephritis (II)	123.2	Ro, Sm, RNP	52/< 5/26	2560	5	10→0	15→0	MCR
2	21 F	84	12.5	IVCY, MTX	CNS	1.4	Ro, RNP	105/19/49	320	6	3→0	15→1	MCR
3	20 F	10	25	IVCY	CNS	< 1.0	—	119/24/53	< 40	10	10→0	13→0	MCR
4	41 F	324	60	IVCY, PE	CNS, TTP nephritis (IV)	500.6	Sm, RNP	28/< 5/13	10240	9.5	20→0	28→0	MCR
5	32 F	252	60	IVCY	CNS nephritis (IV)	8.4	—	56/12/27	< 40	2	28→2	25→0	MCR
6	29 F	6	30	IVCY	lymphadenopathy	5.4	—	114/18/31	320	7.5	9→17*	12→21*	NCR*
7	17 M	3	30	MMF	nephritis (IV)	6.3	—	103/26/55	< 40	5	18→2	13→0	MCR
8	32 F	108	50	IVCY, CsA, AZA, PE	nephritis (IV)	52.3	Ro, Sm, RNP	90/15/39	640	7	16→0	17→0	MCR
9	16 F	30	20	ICVY, MZ, CsA	nephritis (IV) CNS	610.7	Ro	54/8/25	320	12.5	13→10*	23→13*	NCR*
10	27 F	6	40	IVCY, PE IA	nephritis (IV)	242.1	—	35/< 5/9	1280	2.5	35→4	37→3	MCR

* At relapse. RTX: rituximab; CNS: central nervous system; ANA: antinuclear antibody; SLEDAI: Systemic Lupus Erythematosus Disease Activity Index; BILAG: British Isles Lupus Assessment Group Activity Index; CS: prednisolone (or equivalent); CY: cyclophosphamide; IVCY: intravenous cyclophosphamide pulse therapy; CsA: cyclosporin; MZ: mizoribine; PE: plasma exchange; IA: immune adsorption; AZA: azathioprine; MMF: mycophenolate mofetil; TTP: thrombotic thrombocytopenic purpura; ENA: extractable nuclear antigen; AIHA: autoimmune hemolytic anemia; MCR: major clinical response; NCR: no clinical response.

FITC-labeled mouse $IgG_1\kappa$, FITC-conjugated anti-CD40, FITC-conjugated anti-CD80, FITC-conjugated anti-CD69, FITC-conjugated anti-CD45RA, phycoerythrin (PE)-conjugated anti-IgD, PE-conjugated anti-CD45RO, PE-conjugated anti-inducible costimulator (ICOS), PE-Cy5-conjugated anti-CD4, PE-Cy7-conjugated anti-CD19 (Pharmingen, San Diego, CA, USA), FITC-conjugated anti-CD40L (Ancell, Bayport, MN, USA), and allophycocyanin-conjugated anti-CD27 (BioLegend, San Diego, CA, USA). They were then incubated 30 minutes at 4°C, and the cells were washed 3 times with FACS solution and analyzed using the FACSCalibur (Becton-Dickinson, San Jose, CA, USA) and FlowJo software (Digital Biology, Tokyo, Japan). The numbers of CD40 and CD80 molecules expressed per CD19-positive cell were counted using QIFIKIT Beads (Dako Japan, Kyoto, Japan).

Statistical analysis. The results were analyzed using SPSS version 16. The statistical significance of differences between the pretreatment and post-treatment values was tested by Wilcoxon's test. P values < 0.05 were considered statistically significant.

RESULTS

Changes in levels of B cell and T cell surface antigens following rituximab treatment. We analyzed longitudinally the pattern of B cell and T cell differentiation and the changes in the expression levels of the costimulatory molecules on these cells in the longterm responders to rituximab therapy. Figures 1A and 1B show a representative patient with longterm remission after the treatment (Patient 7). Rituximab treatment resulted in a disappearance of CD19+IgD+CD27– naive B cells, CD19+IgD–CD27– memory B cells, and CD19+IgD–CD27+ class-switched memory cells from the peripheral blood within 28 days after treatment. On the other hand, $CD19^{low}CD27^{high}$ or IgD–CD38+ plasma cells persisted in the peripheral blood of these patients until Day 28, although these cells also disappeared completely from the peripheral blood by 6 months after rituximab treatment. The naive B cells recovered within 3 to 9 months after treatment, while the memory B cells and plasma cells remained depleted for 2 years. The similar changes of B cell phenotype were observed in all of the 8 patients with longterm remission of SLE (Figure 1C, 1D). The ritux-

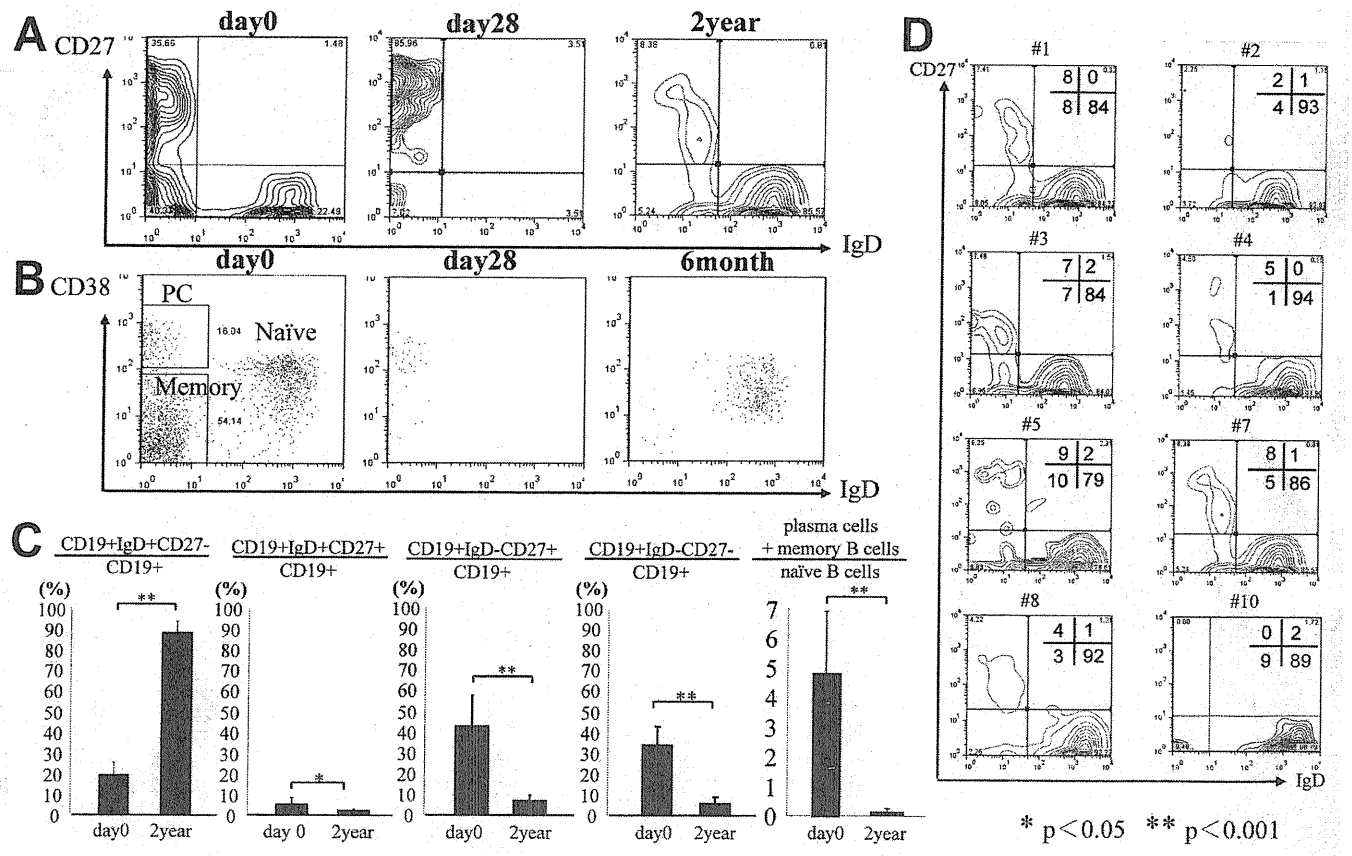

Figure 1. Changes in CD19-positive cell subsets in cases of SLE showing prolonged remission and major clinical response following rituximab therapy. (A) B cell subsets immediately before, 28 days after, and 2 years after rituximab treatment in Patient 7 (a representative case following a typical course). Left upper quadrant identified plasma cells (CD27++) and class-switched memory B cells (CD27+). Right upper quadrant identified IgM memory B cells. Left lower quadrant identified double-negative memory B cells. Right lower quadrant identified naive B cells. (B) B cell subsets and plasma cells immediately before, 28 days after, and 6 months after rituximab treatment in Patient 7 (a case following a typical course). IgD–CD38+ cells show plasma cells. IgD–CD38– cells show memory B cells. IgD+CD38+ cells show naive B cells. (C) Changes in percentages of CD19+IgD+CD27– naive B cells, CD19+IgD+CD27+ IgM memory B cells, CD19+IgD–CD27+ class-switched memory B cells, CD19+IgD–CD27– (double-negative) memory B cells among the CD19-positive cells and the ratio of plasma cells plus memory B cells to naive B cells immediately before and 2 years after rituximab treatment in 8 patients with prolonged remission. (D) CD19-positive cell subset in 8 patients at 2 years.

imab therapy resulted, by 2 years after treatment, in a significant fall in the percentage of CD19+IgD+CD27+ memory B cells (3.0 ± 1.8% to 1.2 ± 0.7%, p < 0.05; 1.0 ± 0.8 cells/μl to 0.9 ± 0.9 cells/μl, p = 0.8203), CD19+IgD–CD27+ class-switched memory B cells (43.5 ± 10.0% to 5.4 ± 3.2%, p < 0.001; 22.8 ± 24.4 cells/μl to 6.7 ± 5.9 cells/μl, p = 0.1187), and CD19+IgD– CD27– memory B cells (34.7 ± 8.8% to 5.9 ± 3.2%, p < 0.001; 14.7 ± 11.0 cells/μl to 5.8 ± 5.9 cells/μl, p = 0.1096); and a significant reduction of the plasma cells and memory B cells/naive B cells ratio (4.80 ± 2.12 to 0.15 ± 0.07, p < 0.001; 4.8 ± 2.1 to 0.1 ± 0.2, p < 0.001).

Next, we assessed the effects of rituximab treatment on the expression levels of costimulatory molecules on CD19-positive cells. Figure 2A shows the changes of phenotypes in a representative case and similar trends were noted in all of the 8 patients with SLE who showed longterm remission following rituximab therapy (Figure 2B). At 2 years after the initial infusion, no significant change from the baseline level of the percentage and the number of CD40-expressing cells among the CD19-positive cells was observed (88.8 ± 10.6% to 76.4 ± 16.0%, p = 0.0742; 78.5 ± 69.1 cells/μl to 80.1 ± 54.5 cells/μl, p = 0.5212), even though the number of CD40 molecules per CD19-positive cell had fallen significantly within 28 days after the treatment (from 1957.8 ± 769.6 to 1200.9 ± 120.2 molecules/cell, p = 0.0357). In contrast to CD40, a significant reduction from baseline levels remained at 2 years in the percentage and number of CD80-expressing cells among the CD19-positive cells (55.8 ± 27.3% to 10.0 ± 5.4%, p = 0.0008; 46.8 ± 29.0 cells/μl to 8.9 ± 9.3 cells/μl, p = 0.0042) and in the number of CD80 molecules per CD19-positive cell (1657.2 ± 1936.1 to 158.4 ± 88.4 molecules/cell, p = 0.0016), indicating the reduction of memory B cells, since CD80 is expressed only on memory B cells.

On the other hand, the percentage of CD4+CD45RO^{bright} memory T cells in the peripheral blood was high before the start of rituximab therapy, and a similar trend was observed until Day 28 in a representative case of Patient 4 (Figure 3A), and similar trends were observed among 8 patients

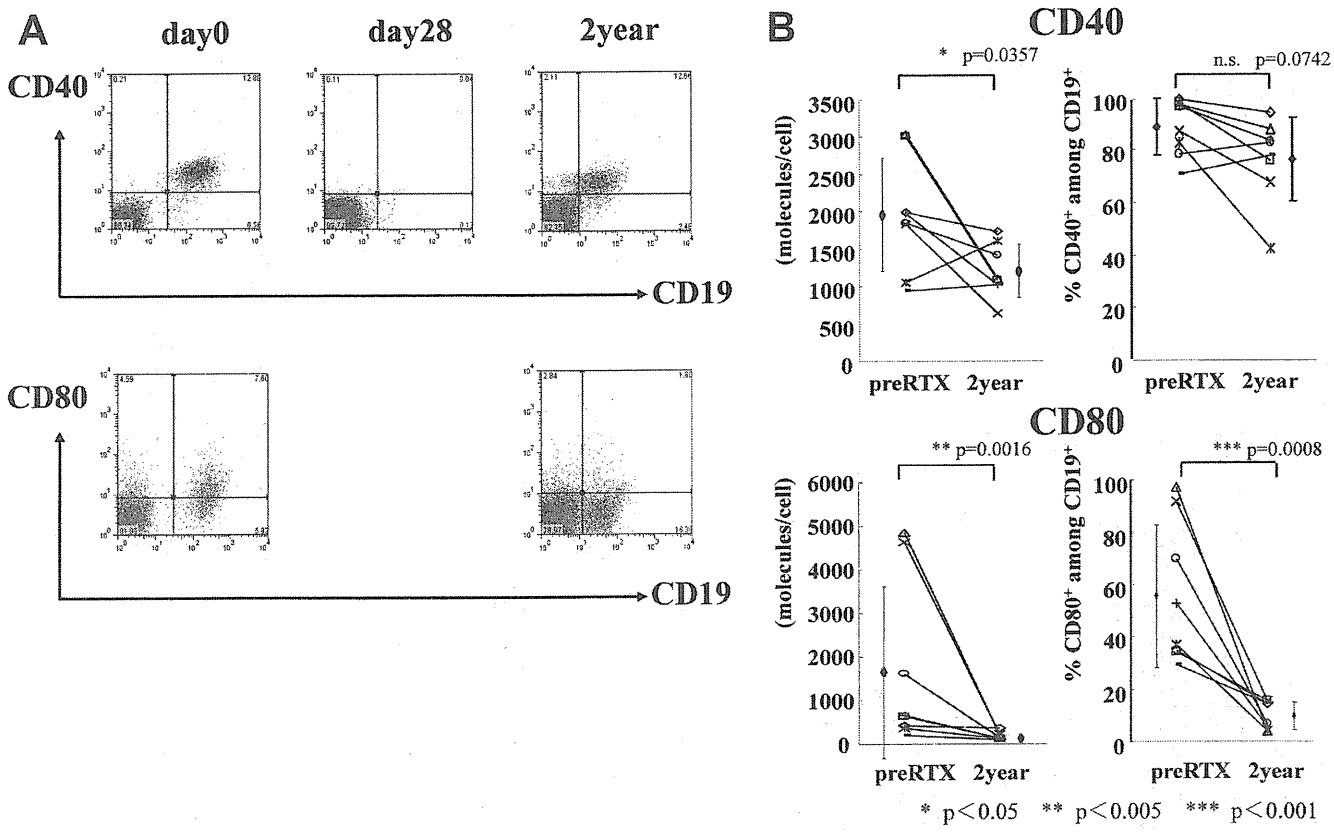

Figure 2. Sequential changes in levels of CD40 and CD80, costimulatory molecules expressed on CD19-positive cells, in patients with SLE who have prolonged remission and show major clinical response following rituximab treatment. (A) Course from immediately before rituximab treatment to 28 days after and 2 years after treatment in representative Patient 7, who followed a typical course (x axis, CD19; y axis, CD40 in the upper panel, CD80 in the lower panel). (B) Changes in the number of CD40 and CD80 molecules per CD19-positive cell (left, using QIFIKIT Beads) and the percentage of CD40-positive and CD80-positive cells among the CD19-positive cells (right) before and 2 years after rituximab treatment in the 8 patients with prolonged remission. RTX: rituximab; n.s.: nonsignificant.

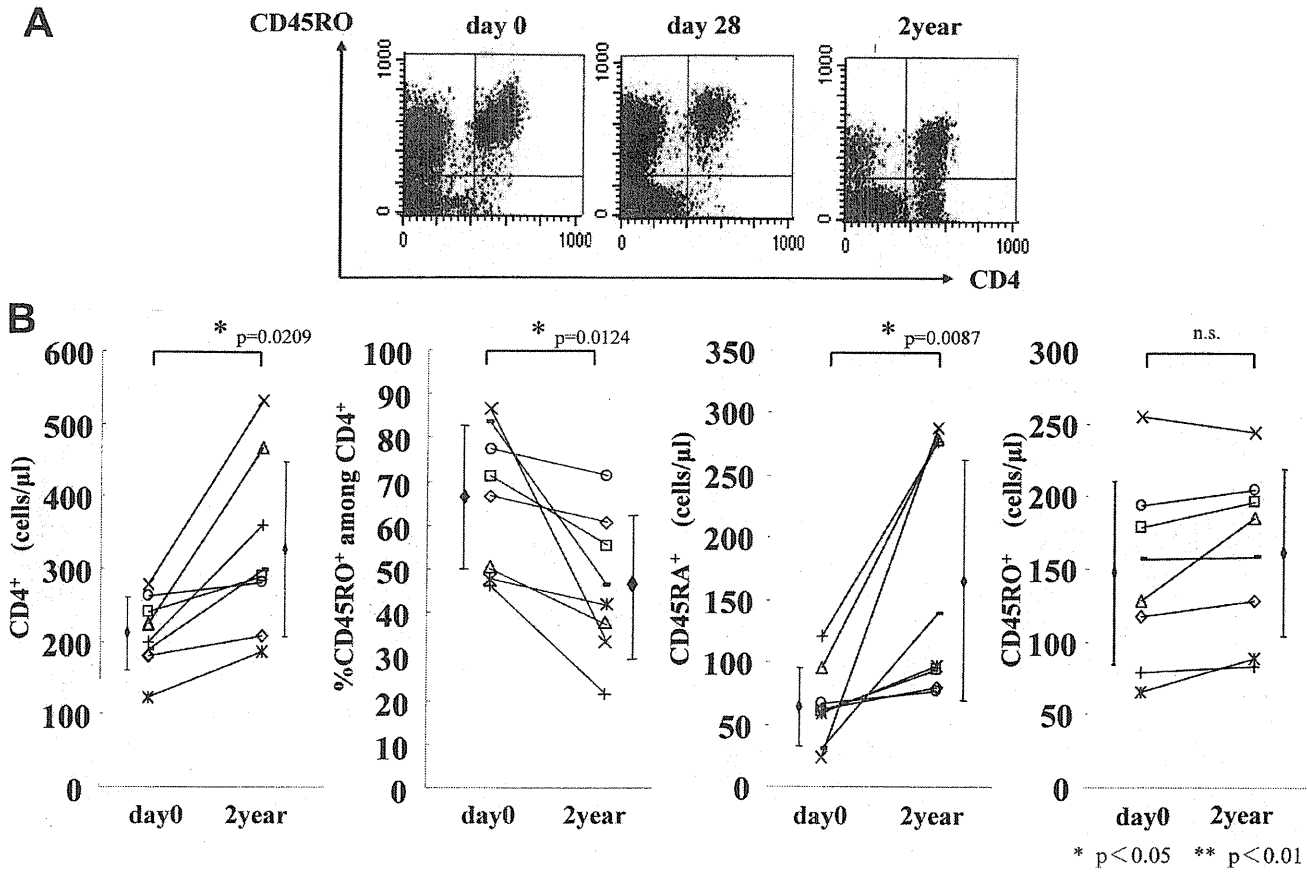

Figure 3. Changes in T cell subsets in patients with SLE with long-sustained remission and major clinical response following rituximab treatment. (A) Course of a representative Patient 4 (x axis, CD4; y axis, CD45RO). The percentage of CD4+CD45RO^{bright} memory cells was high before rituximab treatment and remained high until Day 28 after treatment. After 2 years, however, the level of this costimulatory molecule decreased (CD45RO^{bright} to CD45RO^{intermediate}), along with an increase in the number of CD45RO-negative naive T cells. (B) Changes from baseline to 2 years after treatment in the 8 patients with prolonged remission. From left to right, changes in the actual number of CD4-positive cells, percentage of CD45RO-positive cells among the CD4-positive cells, actual number of CD4+CD45RA+ cells, and the actual number of CD4+CD45RO+ cells are shown.

treated with rituximab (Figure 3B). At 2 years after initial infusion, a significant reduction was observed in the percentage of memory T cells among the CD4-positive T cells (66.2 ± 16.2% to 45.9 ± 16.2%, p = 0.0124) and a significant increase in the number of naive T cells (64.6 ± 31.6 to 165.8 ± 97.2 cells/μl, p = 0.0087). Further, the expression of CD69, an activation marker expressed on CD4-positive cells, and of the costimulatory molecules CD40L and inducible costimulator decreased rapidly by Day 28 in a representative patient (Figure 4A). Expression of these molecules remained reduced for 2 years in 8 patients treated with rituximab (CD69, 17.9 ± 18.7% to 3.8 ± 5.7%, p = 0.0117; 30.5 ± 34.3 cells/μl to 12.1 ± 17.3 cells/μl, p = 0.032; CD40L, 10.0 ± 6.6% to 2.3 ± 1.0%, p = 0.0008; 23.6 ± 21.9 cells/μl to 6.9 ± 2.7 cells/μl, p = 0.0502; and ICOS, 8.7 ± 5.0% to 2.3 ± 1.7%, p = 0.0063; 21.1 ± 10.6 cells/μl to 8.4 ± 7.3 cells/μl, p = 0.0311; Figure 4B).

Changes in expression of lymphocyte surface antigens in patients showing relapse after prolonged remission of SLE. We observed 1 case with B cell-dominant relapse and another with T cell-dominant relapse. The patient with B cell-dominant relapse was a 16-year-old girl (Patient 9) with lupus nephritis (WHO type IV). In this patient, despite intense immunosuppressive therapy, disease activity remained high (SLEDAI 13 and BILAG 23). She achieved remission of SLE after rituximab treatment, with rapid disappearance of the CD19+IgD–CD27– memory B cells and CD19+IgD–CD27+ class-switched memory B cells from the peripheral blood by Day 28, along with rapid reduction in the expression of the costimulatory molecules CD40L and ICOS on the T cells. However, the disease relapsed at 1.5 years after rituximab treatment, and simultaneously the butterfly rash reappeared, the anti-dsDNA antibody titer increased again, and proteinuria recurred. Just before relapse, the percentages of CD19+IgD–CD27– memory B cells and CD19+IgD–CD27+ class-switched memory B